Journal of Theoretical Biology 324 (2013) 52–71

Contents lists available at SciVerse ScienceDirect

Journal of Theoretical Biology

journal homepage: www.elsevier.com/locate/yjtbi

From individuals to populations to communities: A dynamic energy budget model of marine ecosystem size-spectrum including life history diversity

Olivier Maury [a,b,*], Jean-Christophe Poggiale [c,1]

[a] Institut de Recherche pour le Développement (IRD), UMR 212 EME, CRH, av. Jean Monnet, B.P. 171, 34203 Sète cedex, France
[b] International laboratory ICEMASA, Department of Oceanography, University of Cape Town, Private Bag X3, Rondebosch 7701, Cape Town, South Africa
[c] Aix-Marseille University, Université du Sud Toulon-Var, CNRS/INSU, IRD, MIO, UM 110, 13288, Marseille, Cedex 09, France

HIGHLIGHTS

- We develop a DEB-based model of the size-structured dynamics of marine communities.
- It links mechanistically individual, population and community levels.
- It represents an infinite number of interacting species from small to large ones.
- Simulations show that small and large species dominate the community successively.
- The modeled community spectrum is quasi-linear and matches well empirical studies.

GRAPHICAL ABSTRACT

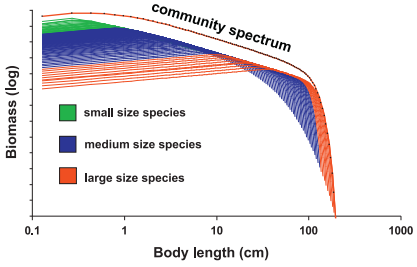

ARTICLE INFO

Article history:
Received 16 September 2011
Received in revised form
14 January 2013
Accepted 24 January 2013
Available online 8 February 2013

Keywords:
Size spectrum
Dynamic Energy Budget theory
Biodiversity
Schooling
Predation

ABSTRACT

Individual metabolism, predator–prey relationships, and the role of biodiversity are major factors underlying the dynamics of food webs and their response to environmental variability. Despite their crucial, complementary and interacting influences, they are usually not considered simultaneously in current marine ecosystem models. In an attempt to fill this gap and determine if these factors and their interaction are sufficient to allow realistic community structure and dynamics to emerge, we formulate a mathematical model of the size-structured dynamics of marine communities which integrates mechanistically individual, population and community levels. The model represents the transfer of energy generated in both time and size by an infinite number of interacting fish species spanning from very small to very large species. It is based on standard individual level assumptions of the Dynamic Energy Budget theory (DEB) as well as important ecological processes such as opportunistic size-based predation and competition for food. Resting on the inter-specific body-size scaling relationships of the DEB theory, the diversity of life-history traits (i.e. biodiversity) is explicitly integrated. The stationary solutions of the model as well as the transient solutions arising when environmental signals (e.g. variability of primary production and temperature) propagate through the ecosystem are studied using numerical simulations. It is shown that in the absence of density-dependent feedback processes, the model exhibits unstable oscillations. Density-dependent schooling probability and schooling-dependent predatory and disease mortalities are proposed to be important stabilizing factors allowing stationary solutions to be reached. At the community level, the shape and slope of the obtained quasi-linear stationary spectrum matches well with empirical studies. When oscillations of primary

* Corresponding author at: International laboratory ICEMASA, Department of Oceanography, University of Cape Town, Private Bag X3, Rondebosch 7701, Cape Town, South Africa.
Tel.: +27 21 650 3279; fax: +27 21 650 3979.
E-mail addresses: Olivier.Maury@ird.fr (O. Maury), jean-christophe.poggiale@univmed.fr (J.-C. Poggiale).
[1] Tel./fax: +33 4 91 82 91 19.

http://dx.doi.org/10.1016/j.jtbi.2013.01.018

production are simulated, the model predicts that the variability propagates along the spectrum in a given frequency-dependent size range before decreasing for larger sizes. At the species level, the simulations show that small and large species dominate the community successively (small species being more abundant at small sizes and large species being more abundant at large sizes) and that the total biomass of a species decreases with its maximal size which again corroborates empirical studies. Our results indicate that the simultaneous consideration of individual growth and reproduction, size-structured trophic interactions, the diversity of life-history traits and a density-dependent stabilizing process allow realistic community structure and dynamics to emerge without any arbitrary prescription. As a logical consequence of our model construction and a basis for future studies, we define the function Φ as the relative contribution of each species to the total biomass of the ecosystem, for any given size. We argue that this function is a measure of the functional role of biodiversity characterizing the impact of the structure of the community (its species composition) on its function (the relative proportions of losses, dissipation and biological work).

1. Introduction

Marine ecosystems are submitted to strong anthropogenic pressures, directly through the effects of fisheries, pollutions and ocean acidification and indirectly through the effects of climate changes and their interaction with natural climate variability. Understanding and predicting those effects and their potential consequences on the services that ecosystems provide to humanity is of major and urgent importance. Amongst the major impediments that should be overcome to answer this need, the links between individual energetic, population dynamics and the functional role of biological diversity at the community level are of critical importance. Addressing those issues requires to link individual, population and community into a unique mechanistic framework. Current efforts to model marine ecosystems can be schematically classified into two categories. First, species based models (e.g. Polovina, 1984; Walters et al., 1997; Pauly et al., 2000; Fulton et al., 2004) where a large number of unstructured species/populations interact through prescribed predator–prey relationships and are represented with no explicit consideration of the physiology and life history of individuals. They thus neglect important phenomenon such as the importance of size in controlling metabolism (Gillooly et al., 2001), predator–prey interactions (Shin and Cury, 2004) and life-history omnivory (i.e. diet changes when organisms grow) (Walters and Kitchell, 2001; Abrams, 2011; Hartvig et al., 2011). Second, size-spectrum models where size rather than taxonomic identity is considered as the major determinant of trophic interactions and metabolism along which the ecosystem dynamics is projected "from bacteria to whales" disregarding the metabolic and physiological differences between species (e.g. Platt and Denman, 1978; Silvert and Platt, 1978, 1980; Dickie et al., 1987; Cushing, 1992; Platt and Denman, 1997; Arino et al., 2004; Benoit and Rochet, 2004; Maury et al., 2007a, 2007b; Blanchard et al., 2009). Most previous attempts to derive size spectrum from mass balance equations were based on mean rates. They were thus neglecting the diversity of life histories in the community (Arino et al., 2004; Benoit and Rochet, 2004; Maury et al., 2007a, 2007b; Blanchard et al., 2009). A few recent studies have attempted to integrate life history differences between species into size-spectrum models at a steady state (Thygesen et al., 2005; Andersen and Beyer, 2006; Andersen et al., 2009) or dynamically (Shin and Cury, 2004; Hartvig et al., 2011) but based on empirical allometric arguments.

In the present paper, we use a trait-based approach (Andersen and Beyer, 2006; Bruggeman and Kooijman, 2007; Follows et al., 2007) to derive mechanistically the dynamic size-spectrum of a generic marine community of consumer organisms from the Dynamic Energy Budget (Kooijman, 2000, 2010; Nisbet et al., 2000; Sousa et al., 2010) of species-specific individuals. This implies three steps. First, a generic DEB model is expressed to describe the bioenergetics of any individual of any given species all along its life cycle. In the framework of the DEB theory, maximum size captures mechanistically most of the interspecific differences of metabolism and life history (Kooijman, 1986). This allows all the parameters of the individual model to be expressed as simple functions of the maximum size of the considered species. Second, the corresponding physiologically structured species-specific population dynamics model (Metz and Dieckman, 1986; Tuljapurkar and Caswell, 1997; De Roos, 1997; Kooi and Kelpin, 2003; Nisbet and Mc Cauley, 2010) is derived from the individual model and simplified. Maximum species size is considered to be a continuous variable so that the population dynamics of all the possible species in the community can be expressed with the same population model and species-specific populations can be related to each other through opportunistic size-based trophic interactions. Finally, the system is integrated both analytically and numerically along the maximum size dimension to infer the emerging dynamics of the community. The stationary solutions of the model as well as the transient solutions arising when environmental signals (e.g. variability of primary production and temperature) propagate through the ecosystem are studied using numerical simulations.

2. Methods

Ecosystems include producers (autotrophic organisms) which convert solar energy and mineral nutrients into biomass, consumers (heterotrophic organisms) which gain energy solely by predation and decomposers which gain energy by turning dead organic material back into mineral nutrients. The present study focuses on consumers. Decomposers are ignored and primary producers, which are not the subject of the paper but are needed to provide food to the consumers, are treated non-mechanistically as a simple "source term".

2.1. Population dynamics of producers

Producers are represented roughly, avoiding an explicit modeling of their growth and reproduction. For that purpose, the dynamics of their total biomass (expressed in term of energy) is simply assumed to follow a logistic equation distributed over the range of structural volume of producers $[V_0, V_1]$ according to a power law with a constant exponent -1 (e.g. Sheldon et al., 1972). Accordingly, the size-dependent dynamics of producers is expressed as follows:

$$\begin{cases} \Gamma_t^p = \int_{V_0}^{V_1} \widehat{\xi}_{t,V}^p dV = V\widehat{\xi}_{t,V}^p \ln\left(\frac{V_1}{V_0}\right) \\ \frac{d\,\widehat{\xi}_{t,V}^p}{dt} = \frac{\widehat{\xi}_{t,V}^p}{\Gamma_t^p}\frac{d\Gamma_t^p}{dt} = \frac{1}{V\ln\left(\frac{V_1}{V_0}\right)}\left(\dot{r}_p\Gamma_t^p\left(1-\frac{\Gamma_t^p}{pcc_t}\right) - \int_{V_0}^{V_1} \dot{\lambda}_{t,V}^p \widehat{\xi}_{t,V}^p dV\right) \end{cases} \quad \forall V \in [V_0; V_1] \tag{1}$$

with $\widehat{\xi}^{p}_{t,V}$ (J cm^{-3} m^{-3}) being the distribution function of the energy content of the producer population at time $t \in [0, +\infty]$, volume of structure V, in 1 m^3 of seawater, Γ^{p}_{t} (J m^{-3}) being the total energy content of the producer population at time t in 1 m^3 of seawater, V_0 and V_1 being respectively the minimum and the maximum structural volume of producers, $\dot{r}_p$ (s^{-1}) being the growth rate of the producer population, pcc_t (J m^{-3}) being a time-dependent forcing function representing the producers carrying capacity which is either constant or sinusoidal and $\dot{\lambda}^{p}_{t,V}$ (s^{-1}) being the predatory mortality rate affecting producers at time t and structural volume V (see Eq. (13) and Appendix D for the expression of predatory mortality).

2.2. Dynamic energy budget of consumer organisms at the individual level

2.2.1. Energy fluxes

The Dynamic Energy Budget (DEB) theory (e.g. Kooijman, 2000, 2010) describes mechanistically the physiological processes involved in the acquisition and use of energy by individual organisms. The energetics of individuals are represented using three state variables: energy stored in the reserve compartment E (J), structural volume V (cm^3) and energy stored in the reproductive buffer E_R (J). Energy fluxes between those compartments are made explicit through the use of powers $\dot{p}$ (J s^{-1}) (see Fig. 1). For any given individual of species k, energy in food is ingested ($\dot{p}^{k}_{X}$) and assimilated ($\dot{p}^{k}_{A}$) by organisms before being stocked into reserves. Reserves are mobilized ($\dot{p}^{k}_{C}$) and a fixed fraction κ of the energy utilized from reserves is allocated to growth of structural material ($\dot{p}^{k}_{G}$) and somatic maintenance ($\dot{p}^{k}_{M}$), the remaining fraction $1-\kappa$ being devoted to maturity maintenance ($\dot{p}^{k}_{J}$) and development or reproduction ($\dot{p}^{k}_{R}$). Only a fraction κ_R of the energy in E_R is turned into eggs reserve.

Table 1 provides the mathematical formulation of all the basic DEB powers as a function of the state variables E and V and the primary DEB parameters defined in Table 1. By convention, [ ] stands for volumetric concentrations and { } for surface-specific concentrations so that $[E]=E/V$ and $\dot{p}^{k}_{X}=\left\{\dot{p}^{k}_{X}\right\}V^{2/3}$ for instance (Kooijman, 2000). All the rates have a dot like $\dot{\rho}$ to indicate the dimension "per time".

Maturity is supposed to occur after a fixed investment into development. If the maturity maintenance rate is equal to the structural maintenance rate ($\dot{p}^{k}_{M}=\dot{p}^{k}_{J}$), as assumed here, this implies that the structural volume at puberty is proportional to the species-specific maximal structural volume V^{k}_{m} as $V^{k}_{p}=\alpha_p V^{k}_{m}$ with α_p being a constant independent of the species k (Kooijman, 2010).

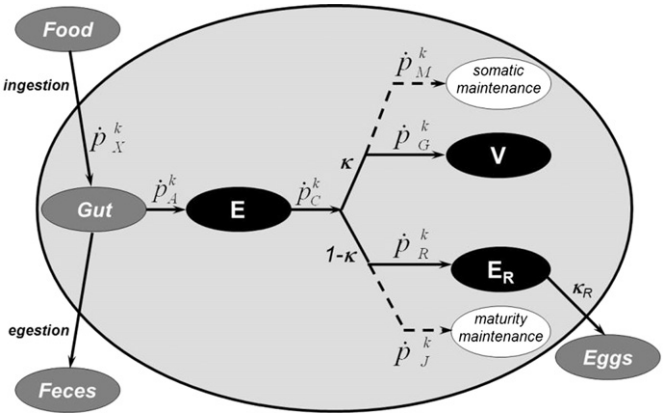

Fig. 1. State variables (black compartments) and energy fluxes (arrows) involved in the bioenergetics of any individual organism of species k in the framework of the DEB theory (see text for details).

Table 1
formulation of the DEB powers used in the present study as a function of the state variables E and V and the primary DEB parameters (cf. Table 1) (from Kooijman, 2000).

Fluxes (J s^{-1})	Formulation
Ingestion	$\dot{p}^{k}_{X}=\{\dot{p}^{k}_{Xm}\}f^{k}V^{2/3}$
Assimilation	$\dot{p}^{k}_{A}=\kappa_X\dot{p}^{k}_{X}=\{\dot{p}^{k}_{Am}\}f^{k}V^{2/3}$
Catabolic	$\dot{p}^{k}_{C}=\frac{[E]}{[E^{k}_{G}]+\kappa[E]}\left(\left[E^{k}_{G}\right]\nu V^{2/3}+[\dot{p}_M]V\right)$
Structural maintenance	$\dot{p}^{k}_{M}=[\dot{p}_M]V$
Structural growth	$\dot{p}^{k}_{G}=\kappa\dot{p}^{k}_{C}-\dot{p}^{k}_{M}$
Maturity maintenance	$\dot{p}^{k}_{J}=\frac{1-\kappa}{\kappa}[\dot{p}_M]\min(V,V^{k}_{p})$
Reproduction	$\dot{p}^{k}_{R}=(1-\kappa)\dot{p}^{k}_{C}-\dot{p}^{k}_{J}$
	$=(1-\kappa)\left[\frac{[E]}{[E_G]+\kappa[E]}([E_G]\nu V^{2/3}+[\dot{p}_M]V)-\frac{[\dot{p}_M]V^{k}_{P}}{\kappa}\right]$

2.2.2. Temperature effect on physiological rates

Due to its major importance in controlling chemical reactions, temperature strongly influences metabolic rates of living organisms (Clarke and Johnston, 1999; Kooijman, 2000; Pörtner, 2002; Clarke, 2004; Speakman, 2005). Despite its purely molecular basis, the description of Arrhenius's based on the van't Hoff equation fits well temperature effects on the physiological rates of organisms at the individual, population and community levels (Kooijman, 2000; Clarke and Fraser, 2004). Such effects are especially important to take into account given that most marine organisms are poikilotherms and hence their internal temperature varies dramatically according to changes in ambient water temperature and metabolic activity. The Arrhenius equation does not keep a mechanistic meaning at the individual level and furthermore at the population and community levels (Clarke, 2004; Clarke and Fraser, 2004). However, it still provides a good statistical description of temperature effects on metabolic rates, even if purely chemical effects are altered by complex processes acting at these scales (Clarke and Johnston, 1999; Gillooly et al., 2001, 2002; Enquist et al., 2003; Clarke, 2004; Clarke and Fraser, 2004). In our model, the Arrhenius temperature-dependent correction factor is used to correct the DEB primary parameters representing metabolic rates ($\{\dot{p}^{k}_{Xm}\}$ and $[\dot{p}_M]$) as well as the probability of disease $\dot{z}$ and the swimming speed. The Arrhenius factor is expressed as follows:

$$\dot{\rho}(T)=\dot{\rho}(T_{ref})e^{\left(\frac{T_A}{T_{ref}}-\frac{T_A}{T}\right)} \quad (2)$$

with $\dot{\rho}$ being the temperature-dependent rate, T being the temperature (K), T_{ref} (K), the reference temperature and T_A (K), a parameter (the "Arrhenius temperature" which equals E_a the activation energy divided by R the gas constant).

2.3. From one individual to a population of consumers

In this section we derive mechanistically a DEB based physiologically structured population dynamics model (Metz and Dieckman, 1986; Tuljapurkar and Caswell, 1997; De Roos, 1997; Kooi and Kelpin, 2003; Nisbet and Mc Cauley, 2010) for any given consumer species k from the individual DEB presented in Section 2.2. Such models link the individual level (i-level) to the population level (p-level) and hence enable to explicitly include the diversity of individual physiological states into the population dynamics. The bio-ecological processes considered are predation, mortality, ingestion, assimilation, storage into reserves and use of energy for maintenance, growth, development and reproduction.

2.3.1. Definitions

A given species k is characterized by its maximal structural volume V_m^k (cm^3) at food saturation which is, for simplifying the notations, noted k. $k \in [V_m^{k_{min}}, V_m^{k_{max}}]$ with $V_m^{k_{min}}$ and $V_m^{k_{max}}$ being the maximal structural volume of respectively the smallest and the largest species in the considered community. The structural volume at birth (hatching) of species k is noted V_b^k (cm^3). We neglect the embryonic phase so that, for any given species k, the structural volume V (cm^3) belongs to $[V_b^k, k]$. The structural volume is supposed to be proportional to the cubed length of organisms $V=(\delta l)^3$ with δ being a constant shape parameter which we assume to be species-independent in a given community. The energy in the reserve compartment of species k belongs to $[0, E_m^k]$ with $E_m^k = k\left[E_m^k\right]$, $\left[E_m^k\right]$ being the maximal energy density in the reserve compartment of species k (Kooijman, 2000).

The population level state variable (p-state) considered here is $\xi_{t,E,V}^k$ ($J\,cm^{-3}\,J^{-1}\,cm^{-3}\,m^{-3}$), the distribution function of the total (including both reserve and structure) energy content of species k, at time $t \in [0, +\infty]$, energy in the reserve compartment E, volume of structure V, in 1 m^3 of seawater. $\xi_{t,E,V}^k$ is a density with respect to species-specific maximum structural volume, reserve energy, structural volume and seawater volume. Therefore, the total quantity of energy (J) contained by the species $[k, k+dk]$ in the range of structural volume $[V_1, V_2]$ per m^3 of seawater at time t is given by

$$\int_{V_1}^{V_2}\int_0^{E_m^k} \xi_{t,E,V}^k dE dV\ dk \tag{3}$$

From $\xi_{t,E,V}^k$ one can define $N_{t,E,V}^k$ ($cm^{-3}\,J^{-1}\,cm^{-3}\,m^{-3}$), the distribution function of the number of individuals of species k in terms of species-specific maximum structural volume, reserve energy and structural volume (t, k, E, V) in 1 m^3 of seawater, with

$$\xi_{t,E,V}^k = (E + d\psi V) N_{t,E,V}^k \tag{4}$$

d being the density of structural biomass ($g\,cm^{-3}$) and ψ being the energy content of one unit of structural biomass ($J\,g^{-1}$) which are both supposed to be constant in time according to the strong homeostasis hypothesis (Kooijman, 2000).

2.3.2. Dynamics for one consumer population

Strictly, a physiologically structured population model based on the unstructured DEB theory should consider at least five dimensions (the dimensions of the i-state vector) plus time (Kooi and Kelpin, 2003): structural volume, amount of energy in the reserve compartment, amount of energy invested into maturation, amount of energy stored in the reproductive buffer and amount of reactive oxydative substances (ROS) in the cells which are responsible for ageing and control aging mortality. However, for the sake of simplicity, we make strong assumptions to limit the number of dimensions of the physiological space to one plus time. These assumptions are:

(1) The assumption that the embryo stage (egg+yolk larvae) can be neglected i.e. that organisms start their life as juveniles (feeding larvae) which start feeding immediately after birth and the assumption that the transition from juveniles to adults (puberty) occurs at fixed sizes proportional to the species-specific maximum sizes. Those assumptions allow to remove from the physiological space the amount of energy invested in maturation which, in the DEB framework, is responsible for lifestage transitions;

(2) The assumption that spawning occurs continuously in time after puberty and that the energy allocated to reproduction is immediately turned into juveniles without being stored allows to remove the reproductive buffer from the physiological space;

(3) The assumption that the ageing mortality rate, which actually depends on the feeding and temperature history of individuals, can be replaced by a mean species-specific ageing mortality curve allows to remove the amount of ROS from the physiological space.

Given those assumptions, the number of dimensions of the physiological space is reduced to two (E and V) and the basic equation used to describe the population dynamics (i.e. the fluxes of individuals of species k through the reserve energy/structural volume space) combines two transport terms for representing the reserve dynamics and the structural growth process and four sink terms for predatory, ageing, starvation and disease mortality processes. It is written as follows for any species k in the domain $[0,E_m^k] \times [V_b,k]$ assuming given initial conditions at $t=0$ and a Dirichlet boundary condition in $V=V_b$ to consider the reproductive input into the population:

$$\begin{cases} \partial_t N_{t,E,V}^k = -\partial_V(\dot\gamma_{t,E,V}^k N_{t,E,V}^k) - \partial_E(\dot\eta_{t,E,V}^k N_{t,E,V}^k) - (\dot\lambda_{t,E,V}^k + \dot a_{t,E,V}^k + \dot s_{t,E,V}^k + \dot z_{t,E,V}^k) N_{t,E,V}^k \\ N_{0,E,V}^k = N_{E,V}^{k,0} \\ \dot\gamma_{t,E,V_b}^k N_{t,E,V_b}^k = \dot r_{t,E}^k \end{cases} \tag{5}$$

where $\dot\gamma$ ($cm^3\,s^{-1}$) is the growth rate of structural volume, $\dot\eta$ ($J\,s^{-1}$) is the rate of change of reserves, $\dot\lambda$ (s^{-1}) is the mortality rate due to predation, $\dot a$ (s^{-1}) is the ageing mortality, $\dot s$ (s^{-1}) is the starvation mortality rate and $\dot z$ (s^{-1}) is the disease mortality rate, $\dot r$ ($cm^{-3}\,J^{-1}\,m^{-3}\,s^{-1}$) is the reproductive input and $N_{E,V}^{k,0}$ the initial state of the system. For all those coefficients, the subscripts k, t, E and V refer respectively to species (maximum structural volume), time, energy in the reserves and volume of structure. Making the extra assumption that

(4) the dynamics of the reserve pool is fast compared to the dynamics of structure and mortality (see Appendix A for the mathematical details about this assumption and its consequences and Appendix B for an analysis of its validity) implies that, at the time scale relevant for population dynamics, the reserve density is always in or near equilibrium. This enables to reduce the reserve energy density distribution to a dirac distribution located on its equilibrium value which equals the scaled functional response times the maximum energy density in the reserves ($[E]^*=f[E_m]$). This allows the removal of the transport term representing the reserve dynamics from Eq. (5).

Removing E^* from the subscripts for clarity, this leads to the following equation of evolution (see Appendix A for its derivation):

$$\begin{cases} \partial_t N_{t,V}^k = -\partial_V(\dot\gamma N_{t,V}^k) - (\dot\lambda_{t,V}^k + \dot a_{t,V}^k + \dot s_{t,V}^k + \dot z_{t,V}^k) N_{t,V}^k \\ N_{0,V}^k = N_V^{k,0} \\ \dot\gamma_{V_b} N_{t,V_b}^k = \dot r(N^k) \end{cases} \tag{6}$$

Eq. (6) is then expressed in term of energy (see Appendix C for the detailed calculations). This leads to

$$\begin{cases} \partial_t \xi_{t,V}^k = -\partial_V(\dot\gamma_{t,V}^k \xi_{t,V}^k) + \frac{\dot\gamma_{t,V}^k \xi_{t,V}^k}{V(d\psi + f_{t,V}[E_m]^k)}(d\psi + [E_m]^k(V\partial_V f_{t,V} + f_{t,V})) \\ \qquad\qquad -(\dot\lambda_{t,V}^k + \dot a_{t,V}^k + \dot s_{t,V}^k + \dot z_{t,V}^k)\xi_{t,V}^k \\ \xi_{0,V}^k = \xi_V^0 \\ \dot\gamma_{t,V_b}^k \xi_{t,V_b}^k = \dot r_t^k \end{cases} \tag{7}$$

The derivation of explicit expressions for all the coefficients of Eq. (7) ($\dot\gamma$, $\dot\lambda$, $\dot a$, $\dot s$, $\dot z$, $\dot r$) is provided in the six sub-sections below.

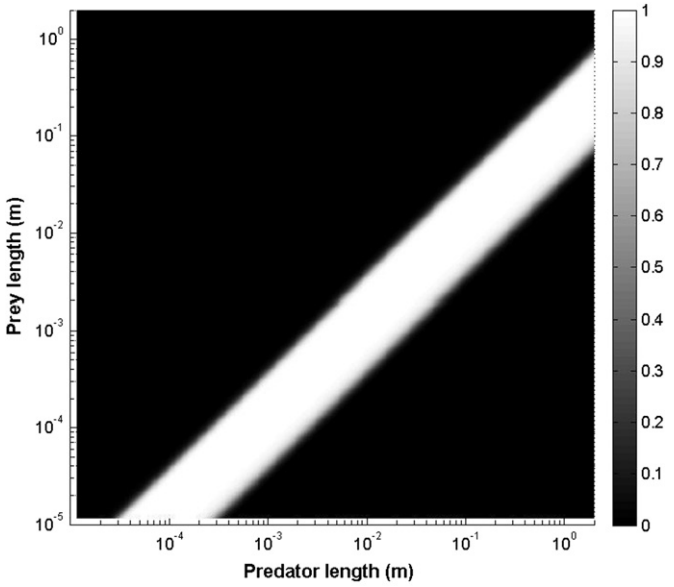

Fig. 2. Selectivity function $s_{u,w}$ versus prey length and predator length.

2.3.2.1. The predation process: calculation of $\dot{\lambda}^{k}_{t,V}$ and $\dot{\lambda}^{p}_{t,V}$. Predation is supposed to be opportunistic and controlled by the ratio of sizes between organisms (all organisms can be potentially predators and preys at the same time, depending on their relative size) and the availability of preys to predators which is supposed to be proportional to their level of local spatial aggregation.

To calculate the quantity of food available to a predator from the density of prey, the size-based constraint on predation is first specified. For that purpose, the selectivity $s_{u,w} \in [0,1]$ is defined as the probability that a consumer organism of structural volume u eats an encountered organism of structural volume w. Assuming that predation can occur if the ratio of predator length over prey length is comprised between two ρ_1 and ρ_2 extreme values, $s_{u,w}$ is a normalized function expressed as the product of two sigmoid functions which account for the limitation of ingestion when preys are either too small or too large (Fig. 2, see Appendix D for the equation of selectivity):

The second constraint on predation, the local level of spatial aggregation of prey, is then specified and linked to the density of prey. Most pelagic organisms exhibit schooling (fish) or swarming (zooplankton) behaviors. It has been shown both theoretically (Vicsek et al., 1995; Czirok and Vicsek, 2000; Tu, 2000) and empirically (Becco et al., 2006) that such aggregative structures appear above a critical organisms density and are not sustained below this threshold. Hence, pelagic populations exhibit phase transitions when this threshold is reached, like many physical systems. This macroscopic phenomenon results from complex auto-organization processes which are beyond the scope of the present work. Here, we assume that schooling/swarming has important consequences on the predation process by allowing prey availability to predators to increase suddenly when prey density reaches a critical level and dense aggregations such as schools and swarms appear.

Assuming that schools are strictly size- and species-specific (Fréon and Misund, 1999) and appear when the biomass contained in a volume proportional to the structural body volume reaches a size- and species-independent constant (Makris et al., 2009), the probability of schooling ps is expressed as follows:

$$ps^{k}_{t,V} = \frac{(V\xi^{k}_{t,V})^{\beta}}{(V\xi^{k}_{t,V})^{\beta} + s^{\beta}_{crit}} \tag{8}$$

With scrit ($J\,J^{-1}\,m^{-3}\,m^{-3}$) being the biomass density threshold above which the probability of schooling is larger than 0.5 and β a constant parameter characterizing the shape of the threshold function.

Given those size- and aggregation-based constraints, the energy content $p_{t,u}$ ($J\,m^{-3}$) of all the prey available (schooled) and selected by predators of structural volume u is expressed as follows:

$$p_{t,u} = \int_{v=V_b^{k\min}}^{V_m^{k\max}} s_{u,v}\left[\int_{k=v}^{V_m^{k\max}} ps^{k}_{t,v}\xi^{k}_{t,v}dk\right]dv + \int_{V_0}^{V_1} s_{u,v}\widehat{\xi}^{p}_{t,v}dv \tag{9}$$

A scaled size-dependent Holling type II functional response without predator interference is assumed. It is calculated as follows for a species k predator of structural volume u:

$$f^{k}_{t,u} = \frac{p_{t,u}}{\dot{c}^{k}/u^{\chi} + p_{t,u}}, \quad R^{+} \xrightarrow{f} [0;1[\tag{10}$$

with $\dot{c}^{k}$ being a constant parameter (searching rate-1) ($J\,s^{-1}$) and u^{χ} the volume of water explored by a predator of structural volume u per unit of time ($m^3\,s^{-1}$) (which is supposed to be proportional to its swimming speed which is proportional to body length – Froese and Pauly, 2000 – hence χ is taken equal to 1/3).

According to the DEB theory, the individual assimilation rate is proportional to the scaled functional response and body surface: $\dot{p}^{k}_{A} = \kappa_X \dot{p}^{k}_{X} = \{\dot{p}^{k}_{Am}\} f^{k} V^{2/3}$ (Table 1). It follows that $E^{k}_{t,u}dk\,du\,dt$ ($J\,m^{-3}$), the total amount of energy preyed by all predators of species comprised in the range $[k, k+dk]$ and structural volume comprised in the range $[u, u+du]$ at time t during dt in 1 m^3 of water, is expressed as

$$\begin{aligned} E^{k}_{t,u}dk\,du\,dt &= N^{k}_{t,u}\dot{p}^{k}_{X}\,dk\,du\,dt \\ &= N^{k}_{t,u}\frac{\{\dot{p}^{k}_{Am}\}}{\kappa_X} f^{k}_{t,u} u^{1/3}\,dk\,du\,dt \\ &= \frac{\xi^{k}_{t,u}}{d\psi u + E^{k}_{t,u}}\frac{\{\dot{p}^{k}_{Am}\}}{\kappa_X} f^{k}_{t,u} u^{2/3}\,dk\,du\,dt \\ &= \frac{\{\dot{p}^{k}_{Am}\}}{\kappa_X}\,\frac{f^{k}_{t,u}\xi^{k}_{t,u}u^{-1/3}}{d\psi + f^{k}_{t,u}[E^{k}_{m}]}\,du\;dk\;dt \end{aligned} \tag{11}$$

According to the hypothesis of opportunistic predation (preys of a given weight are eaten in proportion to their selected available biomass relatively to the biomass of all possible preys available), the total amount of energy $E^{/q}_{t,/w}\,dq\,dw\,dt$ ($J\,m^{-3}$) preyed by all predators on both all consumer preys of species $[q, q+dq]$ and all producer organisms in the range of structural volume $[w, w+dw]$ at time t during dt in 1 m^3 of water can be calculated (see Appendix D for the details of this calculation) and is used to derive the expression of the instantaneous mortality rate exerted by all predators on species q and structural volume w preys at time t:

$$\dot{\lambda}^{q}_{t,w} = \frac{E^{/q}_{t,/w}}{\xi^{q}_{t,w}} = \frac{ps^{q}_{t,w}}{\kappa_X}\int_{k=V_b}^{V_m^{k\max}}\int_{u=V_b}^{k}\left[\frac{\{\dot{p}^{k}_{Am}\}\xi^{k}_{t,u}u^{-1/3}s_{u,w}}{\frac{ck^{-1/3}d\psi}{u^{\chi}} + (d\psi + [E^{k}_{m}])p_{t,u}}\right]du\;\;dk \tag{12}$$

and the instantaneous mortality rate exerted by all predators on producer organisms of structural volume w at time t:

$$\dot{\lambda}^{p}_{t,w} = \frac{E^{/p}_{t,/w}}{\widehat{\xi}^{p}_{t,w}} = \frac{1}{\kappa_X}\int_{k=V_b}^{V_m^{k\max}}\int_{u=V_b}^{k}\left[\frac{\{\dot{p}^{k}_{Am}\}\xi^{k}_{t,u}u^{-1/3}s_{u,w}}{\frac{ck^{1/3}d\psi}{u^{\chi}} + (d\psi + [E^{k}_{m}])p_{t,u}}\right]du\;\;dk \tag{13}$$

2.3.2.2. The growth process: calculation of $\dot{\gamma}^{k}_{t,V}$. The growth in length cannot be negative for most marine organisms which

have an exo- or an endo-skeleton such as vertebrates, most molluscs, crustaceans, etc. Since the shape parameter δ is supposed to be constant ($V=(\delta l)^3$), the growth of structural volume cannot be negative either (see the paragraph on starvation mortality for the treatment of mass conservation). Using the assumption of fast dynamics of the reserves compared to the dynamics of the structure, the instantaneous growth rate of structural volume can therefore be expressed as

$$\dot{\gamma}^k_{t,V} = \frac{[\dot{p}^k_G]^+}{[E_G]} = \left[\frac{\kappa\{\dot{p}^k_{Am}\}f^k_{t,V}V^{2/3} - [\dot{p}_M]V}{\kappa f^k_{t,V}[E^k_m] + [E_G]}\right]^+ \tag{14}$$

with $[x]^+$ being the function defined by $\begin{cases}[x]^+ = x & if \quad x \geq 0\\ [x]^+ = 0 & if \quad x < 0\end{cases}$ and all the DEB parameters being defined Table 2.

2.3.2.3. The reproduction process: calculation of $\dot{r}^k_t$. For a given species, all size larger than the species-specific size at puberty of both sex are supposed to reproduce permanently but only female sexual products are considered in the reproductive flux. As for the expression of the growth rate and because the contribution to reproduction cannot be negative, the function $[\ ]^+$ is used to express the reproductive input into the system (see the paragraph on starvation mortality for the treatment of mass conservation and the supplementary materials for more details)

$$\dot{r}^k_t = (1-M_{egg})\phi\kappa_R \int_{V^k_p}^{k} N^k_{t,V}[\dot{p}^k_R]^+ dV \tag{15}$$

with $\phi \in [0,1]$ being the sex-ratio in the population supposed to be independent of size, $M_{egg} \in [0;1]$ being the fraction of the spawned eggs which are not fertilized, κ_R being the fraction of the energy in the gonads which is turned into eggs.

After development, Eq. (15) gives

$$\dot{r}^k_t = (1-M_{egg})\phi\kappa_R(1-\kappa)\int_{V^k_p}^{k}\left(\frac{\xi^k_{t,V}}{(f^k_{t,V}[E^k_m]+d\psi)} \times\left[\frac{f^k_{t,V}[E^k_m]([E_G]vV^{-1/3}+[\dot{p}_M])}{[E_G]+\kappa f^k_{t,V}[E^k_m]} - \frac{[\dot{p}_M]V^k_p}{\kappa V}\right]^+\right)dV \tag{16}$$

with $v = \{\dot{p}^k_{Am}\}/[E^k_m]$, the energy conductance ($\mathrm{cm\,s^{-1}}$) which is independent of species (Kooijman, 2000).

2.3.2.4. The starvation mortality: calculation of $\dot{s}^k_{t,V}$. When starvation occurs, i.e. when the food ration is not sufficient to meet organism's needs, growth and/or reproduction cease and structural materials of the body are lysed and used for maintaining the most important physiological functions necessary for survival (Kooijman, 2000). The starvation process leads to a quick weakening of organisms which increases mortality. At the ecosystem level, starvation is a net dissipation of energy. To conserve the mass in a consistent way when growth and/or reproduction cease due to insufficient food intake (cf. Eqs. (14) and (16)), it is considered that the quantity of energy which is needed for maintenance but which cannot be provided by food intake is removed from the ecosystem (Maury et al., 2007a). In this perspective, starvation acts as a mortality term at the level of

Table 2
Designation, dimension, value and source of the parameters used for numerical simulations.

Parameter	Designation	Dimension	Value	Source
DEB parameters				
$\{\dot{p}^k_{Am}\}$	Maximum surface-specific assimilation rate	$\mathrm{J\,m^{-2}\,s^{-1}}$	$\begin{cases}\alpha_{\{\dot{p}_{Am}\}}k^{1/3}\\ \alpha_{\{\dot{p}_{Am}\}} = 22.5\ \mathrm{J\,cm^{-3}\,d^{-1}}\end{cases}$	Kooijman (2010)
$[E^k_m]$	Maximum reserve density	$\mathrm{J\,m^{-3}}$	$\begin{cases}\alpha_{[E_m]}k^{1/3}\\ \alpha_{[E_m]} = 1125\ \mathrm{J\,cm^{-4}}\end{cases}$	Kooijman (2010)
v	Energy conductance	$\mathrm{cm\,s^{-1}}$	$v = \{\dot{p}^k_{Am}\}/[E^k_m] = 0.02\ \mathrm{cm\,d^{-1}}$	Kooijman (2010)
$[\dot{p}_M]$	Maintenance rate	$\mathrm{J\,m^{-3}\,s^{-1}}$	$18\ \mathrm{J\,cm^{-3}\,d^{-1}}$	Kooijman (2010)
$[E_G]$	Volume specific cost of growth	$\mathrm{J\,m^{-3}}$	$2800\ \mathrm{J\,cm^{-3}}$	Kooijman (2010)
V^k_p	Structural volume at puberty	$\mathrm{m^3}$	$\begin{cases}\alpha_p k\\ \alpha_p = 0.38\end{cases}$	Derived from Kooijman (2010)
κ	Fraction of the utilized energy which is allocated to growth and somatic maintenance	/	0.8	Derived from Kooijman (2010)
κ_R	fraction of the energy in the gonads which is turned into eggs	/	0.95	Kooijman, 2010
$\ddot{h}_a$	Ageing acceleration	$\mathrm{s^{-2}}$	$10^{-8}\mathrm{d^{-2}}$	Present study
κ_X	Assimilation efficiency	/	0.8	Maury et al. (2007a)
T_A	Arrhenius temperature	/	8000	Maury et al. (2007a)
δ	Shape coefficient	/	0.2466	Present study
Other parameters				
$\dot{c}$	searching rate^{-1} of the functional response	$\mathrm{J\,s^{-1}}$	1020	Present study
ρ_1	Mean minimum ratio of predator length over prey length	/	3	Maury et al. (2007a)
ρ_2	Mean maximum ratio of predator length over prey length	/	30	Maury et al. (2007a)
α_1	Variability of the minimum ratio of predator length over prey length	/	3	Maury et al. (2007a)
α_2	Variability of the minimum ratio of predator length over prey length	/	0.3	Maury et al. (2007a)
s_{crit}	biomass density threshold above which the probability of schooling is larger than 0.5	$\mathrm{J\,J^{-1}\,m^{-3}\,m^{-3}}$	1022	Present study
β	shape of the probability of schooling function.	/	3	Present study
$\dot{z}$	maximum mortality rate due to disease	$\mathrm{s^{-1}}$	$0.05\ \mathrm{d^{-1}}$	Present study
φ	sex-ratio (mean proportion of females)	/	0.5	Present study
M_{egg}	fraction of the spawned eggs which are not fertilized	/	0	Present study
d	density of biomass	$\mathrm{kg\,m^{-3}}$	$1\ \mathrm{g\,cm^{-3}}$	/
ψ	energy content of biomass	$\mathrm{J\,kg^{-1}}$	$4.103\ \mathrm{J\,g^{-1}}$	Kooijman (2010)
$\dot{r}_p$	Growth rate of the producer population	$\mathrm{s^{-1}}$	$0.5\ \mathrm{d^{-1}}$	Present study
pcc_t	Carrying capacity of the producer population	$\mathrm{J\,m^{-3}}$	$1027\ \mathrm{J\,m^{-3}}$	Present study

the ecosystem and the starvation mortality coefficient can be expressed as follows using Eqs. (14) and (16):

$$\dot{s}^k_{t,V} = \frac{N^k_{t,V}}{\xi^k_{t,V}}([-\dot{p}^k_G]^+ + [-\dot{p}^k_R]^+)$$
$$= \frac{1}{(f^k_{t,V}[E^k_m] + d\psi)}\left([E_G]\left[\frac{[\dot{p}_M] - \kappa\{\dot{p}^k_{Am}\}f^k_{t,V}V^{-1/3}}{[E_G] + \kappa f^k_{t,V}[E^k_m]}\right]^+ + (1-\kappa)\left[\frac{[\dot{p}_M]V^k_p}{\kappa V} - \frac{f^k_{t,V}[E^k_m]([E_G]\nu V^{-1/3} + [\dot{p}_M])}{[E_G] + \kappa f^k_{t,V}[E^k_m]}\right]^+\right) \quad (17)$$

2.3.2.5. The disease mortality: calculation of $\dot{z}^k_{t,V}$. Infectious diseases, either caused by viral, bacterial, protozoan and fungal pathogens or by metazoan parasites, are important components of the ecology of wild marine animals and can have a dramatic negative impact on natural populations (Levy and Wood, 1992). Epizootic are common and often lead to massive mortality levels, causing major losses in populations. It is generally accepted that the prevalence of disease is linked to the spatial density of individuals in a population (Moyle and Cech, 2004; Ogut and Reno, 2004). In the present study we hypothesize that disease mortality acts as a density-dependent phenomenon regulating population densities and stabilizing the overall ecosystem dynamics. In this perspective, we assume that the prevalence of disease and the associated mortality are both proportional to the probability of schooling

$$\dot{z}^k_{t,V} = \dot{z}\, ps^k_{t,V} \quad (18)$$

with $\dot{z}$ (s^{-1}) being a parameter standing for the maximum mortality rate due to disease which is reached when the probability of schooling is one.

2.3.2.6. The ageing mortality: calculation of $\dot{a}^k_{t,V}$. In the framework of the DEB theory, the ageing mortality is assumed to be proportional to the amount of cellular damages. Such damages accumulate at a rate proportional to the amount of DNA lesions which increases at a rate proportional to the intra-cellular concentration of reactive oydative substances (ROS) which is proportional to the respiration rate not associated to assimilation (Kooijman, 2000, 2001, 2010; van Leeuwen et al., 2010). Consequently, the low metabolic rate of large organisms explains that they exhibit much longer life span than small organisms (e.g., Speakman, 2005).

Given this simple set of mechanisms, Kooijman (2000) shows that the ageing mortality (the so-called "hazard rate") can be expressed as follows:

$$a^k_t = \frac{\ddot{h}_a}{V_t}\left(\int_{t_1=0}^{t_1=t} V_{t_1}dt_1 - V_b t + \frac{[\dot{p}_M]}{[E_G]}\int_{t_1=0}^{t_1=t}\int_{t_2=0}^{t_2=t_1} V_{t_2}dt_2dt_1\right) \quad (19)$$

With $\ddot{h}_a$, the ageing acceleration (s^{-2}).

Assuming that the functional response $f^k_{t,V}$ can be replaced by its mean value $\overline{f}^k$ during the time interval [0, t], the mean time taken by an individual of species k to reach size (structural volume) V can be calculated and is used in Eq. (19) to estimate the mean size-dependant ageing mortality rate for species k at size (structural volume) V. Appendix D provides the explicit expression of a^k_V and more details about its derivation.

2.4. From population to community

In this section we use the inter-specific scaling rules of the DEB theory to derive the dynamics of the consumer's community by integrating explicitly the species-specific physiologically structured population dynamics model derived in Section 2.3. over all possible species. The resulting model links the population level (p-level) to the community level (c-level) and explicitly incorporates the diversity of life histories (species) in the community dynamics.

2.4.1. Definitions

To consider the dynamics at the scale of the whole community, we define the aggregated state variable

$$\zeta_{t,E,V} = \int_V^{V^{k\max}_m} \xi^k_{t,E,V}dk \quad (20)$$

which is the distribution function of the total energy content of the consumer community including all the possible species (including both reserve and structure of all the species) ($J\,J^{-1}\,cm^{-3}\,m^{-3}$) at ($t$, E, V) in 1 m^3 of seawater. $\zeta_{t,E,V}$ is independent of k, it is a density with respect to reserve energy, structural volume and seawater volume. Hence, the total quantity of energy contained by all consumer species in the range of structural weight [V_1, V_2] per m^3 of seawater is given by

$$\int_{V_1}^{V_2}\int_0^{k\left[E^k_m\right]} \zeta_{t,E,V}dEdV \quad (21)$$

$\zeta_{t,E,V}$ can easily be converted into the more usual "normalized biomass size-spectrum" using d and ψ assuming that they are both constant parameters over species and sizes.

2.4.2. Dynamics

The dynamics of all the possible species in the community have to be integrated to derive the dynamics of the community. In this perspective, assuming that there is an infinite number of potential life histories (species) in the community, Eq. (7) can be integrated over the range of species larger than V. Using the properties of extensive DEB parameters (Kooijman, 2000) to express $\{\dot{p}^k_{Am}\}$, $[E_m]^k$, $\dot{c}^k$ and V^k_p as functions of the species-specific asymptotic structural volume ($\{\dot{p}^k_{Am}\} = \alpha_{\{\dot{p}_{Am}\}}k^{1/3}$; $[E^k_m] = \alpha_{[E_m]}k^{1/3}$; $\dot{c}^k = \alpha_{\dot{c}}k^{1/3}$; $V^k_p = \alpha_p k$), the dynamics of the whole consumer community can be expressed as follows (see Appendix E for more details about the derivation of this equation):

$$\frac{\partial\zeta_{t,V}}{\partial t} = -\frac{\partial\int_V^{V^{k\max}_m}\dot{\gamma}^k_{t,V}\xi^k_{t,V}dk}{\partial V} + d\psi\int_V^{V^{k\max}_m}\left(\frac{\dot{\gamma}^k_{t,V}\xi^k_{t,V}}{V(d\psi + f^k_{t,V}\alpha_{[E_m]}k^{1/3})}\right)dk + \alpha_{[E_m]}\int_V^{V^{k\max}_m}\left(\frac{\left(V\frac{\partial f^k_{t,V}}{\partial V} + f^k_{t,V}\right)\dot{\gamma}^k_{t,V}k^{1/3}\xi^k_{t,V}}{V(d\psi + f^k_{t,V}\alpha_{[E_m]}k^{1/3})}\right)dk - \int_V^{V^{k\max}_m}(\dot{\lambda}^k_{t,V} + \dot{a}^k_{t,V} + \dot{s}^k_{t,V} + \dot{z}^k_{t,V})\xi^k_{t,V}dk \quad (22)$$

Let us now define the function $\Phi^k_{t,V}$ so that $\begin{cases}\xi^k_{t,V} = \zeta_{t,V}\Phi^k_{t,V}\\ \int_V^{V^{k\max}_m}\Phi^k_{t,V}dk = 1\end{cases}$ (23)

The function $\Phi^k_{t,V}$ expresses the relative contribution of each species k to the total energy content of the ecosystem, for any given structural volume V. Eq. (22) can be expressed using $\Phi^k_{t,V}$ to let the c-level aggregated variable $\zeta_{t,V}$ appear instead of the p-level local variables $\xi^k_{t,V}$

$$\frac{\partial\zeta_{t,V}}{\partial t} = -\frac{\partial\left(\zeta_{t,V}\int_V^{V^{k\max}_m}\dot{\gamma}^k_{t,V}\Phi^k_{t,V}dk\right)}{\partial V} + d\psi\zeta_{t,V}\int_V^{V^{k\max}_m}\left(\frac{\dot{\gamma}^k_{t,V}\Phi^k_{t,V}}{V\left(d\psi + f^k_{t,V}\alpha_{[E_m]}k^{1/3}\right)}\right)dk$$

$$+\alpha_{[E_m]}\zeta_{t,V}\int_V^{V_m^{k\max}}\left(\frac{\left(V\frac{\partial f_{t,V}^k}{\partial V}+f_{t,V}^k\right)\dot{\gamma}_{t,V}^k k^{1/3}\Phi_{t,V}^k}{V\left(d\psi+f_{t,V}^k\alpha_{[E_m]}k^{1/3}\right)}\right)dk$$

$$-\zeta_{t,V}\int_V^{V_m^{k\max}}\Phi_{t,V}^k\left(\dot{\lambda}_{t,V}^k+\dot{a}_{t,V}^k+\dot{s}_{t,V}^k+\dot{z}_{t,V}^k\right)dk \quad (24)$$

With

$$f_{t,V}^{k_1}=\frac{\int_{v=0}^{V_m^{k\max}} s_{u,v}\zeta_{t,v}\left[\int_v^{V_m^{k\max}} ps_{t,v}^k\Phi_{t,v}^k dk\right]dv+\int_{V_0}^{V_1} s_{u,v}\widehat{\xi}_{t,v}^p dv}{\frac{\alpha_c k_1^{1/3}}{u^{\chi}}+\int_{v=0}^{V_m^{k\max}} s_{u,v}\zeta_{t,v}\left[\int_v^{V_m^{k\max}} ps_{t,v}^k\Phi_{t,v}^k dk\right]dv+\int_{V_0}^{V_1} s_{u,v}\widehat{\xi}_{t,v}^p dv} \quad (24)$$

Eq. (24) provides the dynamics of the entire community, integrating the dynamics of every possible single species without making them explicit. An analytical resolution of Eq. (24) is out of reach at present but numerical approximations can be envisioned, using parametric or non-parametric (such as B-splines which would be fitted to empirical data) approximations of the unknown $\Phi_{t,V}^k$ function.

2.5. Numerical approximation

Being coupled, the dynamics of producers and the dynamics of consumers are integrated simultaneously at the *p*-level. A time-splitting method is used for that purpose. Eq. (1), which represents the dynamics of producers, is first integrated numerically using a first order in time semi-implicit scheme (see Appendix F). Semi-implicit numerical schemes improve the stability of the numerical approximation compared to fully explicit methods. Eq. (7) is then integrated numerically forward in time along the species dimension (the maximum structural volume k) and the structural volume V dimension. The same discretization based on 100 logarithmically distributed size classes is used for both dimensions (see Appendix F). A first order upwind finite difference scheme is used for approximating the advection term of Eq. (7) along the V dimension (see Appendix F. All the integrals used in Eq. (F1) and in the calculation of the coefficients of Eq. (F3) are evaluated using simple first order approximations as

$$\int_a^b x dx \approx \sum_{i(a)}^{i(b)} x_i \delta x_i \quad (25)$$

Most of the parameters used in the model are DEB parameters which have a clear physiological significance and are well documented in the literature. Other parameters come from both experimental and theoretical studies. For some secondary parameters however, such as pcc_t, the carrying and r_t, the growth rate of producers biomass, values have been fixed arbitrarily to obtain realistic results. Parameters values used in the simulations are provided in Table 2 with the corresponding references.

2.6. Simulation experiments

All the numerical experiments are conducted using the reference values of the parameters given in Table 2. In a first set of simulations with stable environmental conditions, the existence of a linear steady state is tested by running the models during 100 years for an arbitrary set of 100 species covering the whole range of possible maximum sizes from 1 mm to 2 m.

In a second set of simulations, the non-stationary behavior of the model is studied in the case of environmental variability. For that purpose, sinusoidal oscillations of the carrying capacity of primary producers (100% amplitude) or temperature (10 °C amplitude) are simulated, with 1 and 5 year periodicity.

3. Results

3.1. Steady state

In stable environmental conditions (constant primary production and constant temperature), both the numerical abundance and the biomass of the community converge from any positive initial distribution to a stationary state characterized by non-linear log–log size-spectra (Figs. 3 and 4). For individual species, the spectra in abundance (or biomass) are slightly decreasing (or slightly increasing) until a critical size above which they decrease steadily for a given size range before decreasing sharply for the largest sizes due to the slowdown of growth and the increase of ageing mortality for the largest sizes close to the asymptotic length. The species size-spectra exhibit lower abundance/biomass and the change of slope occur at larger sizes for larger species. At the level of the community, the size spectra are slightly curved (with a very slight increase for the biomass spectra) until 0.45 cm and then exhibit a quasi-linear section in the range $10^{-2}-1$ m before a rapid decrease for large sizes (Figs. 3 and 4).

Fig. 5(a–f) provides the reader with the species-dependent ageing, probability of schooling, predatory and disease mortality

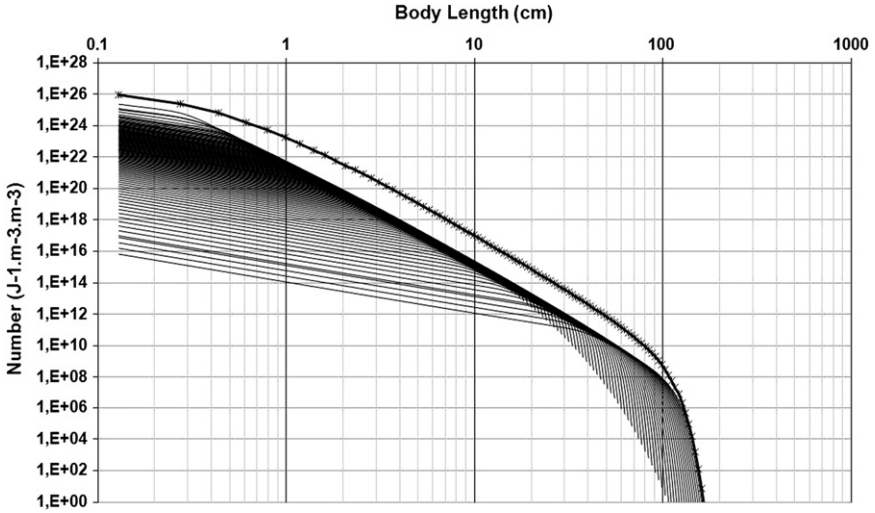

Fig. 3. Stationary size spectrum in numbers (numerical abundance) for the 100 individual species considered (thin lines) and for the community (thick crossed line);

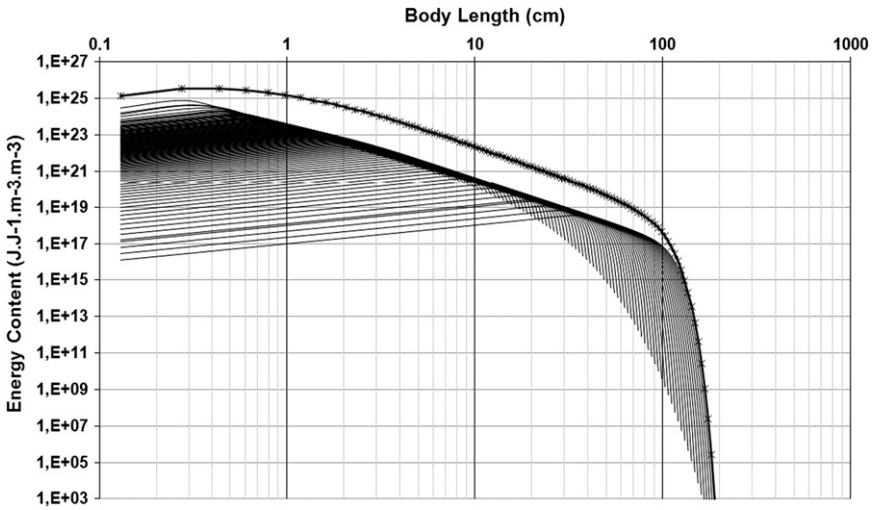

Fig. 4. Stationary size spectrum in biomass for the 100 individual species considered (thin lines) and for the community (thick crossed line);

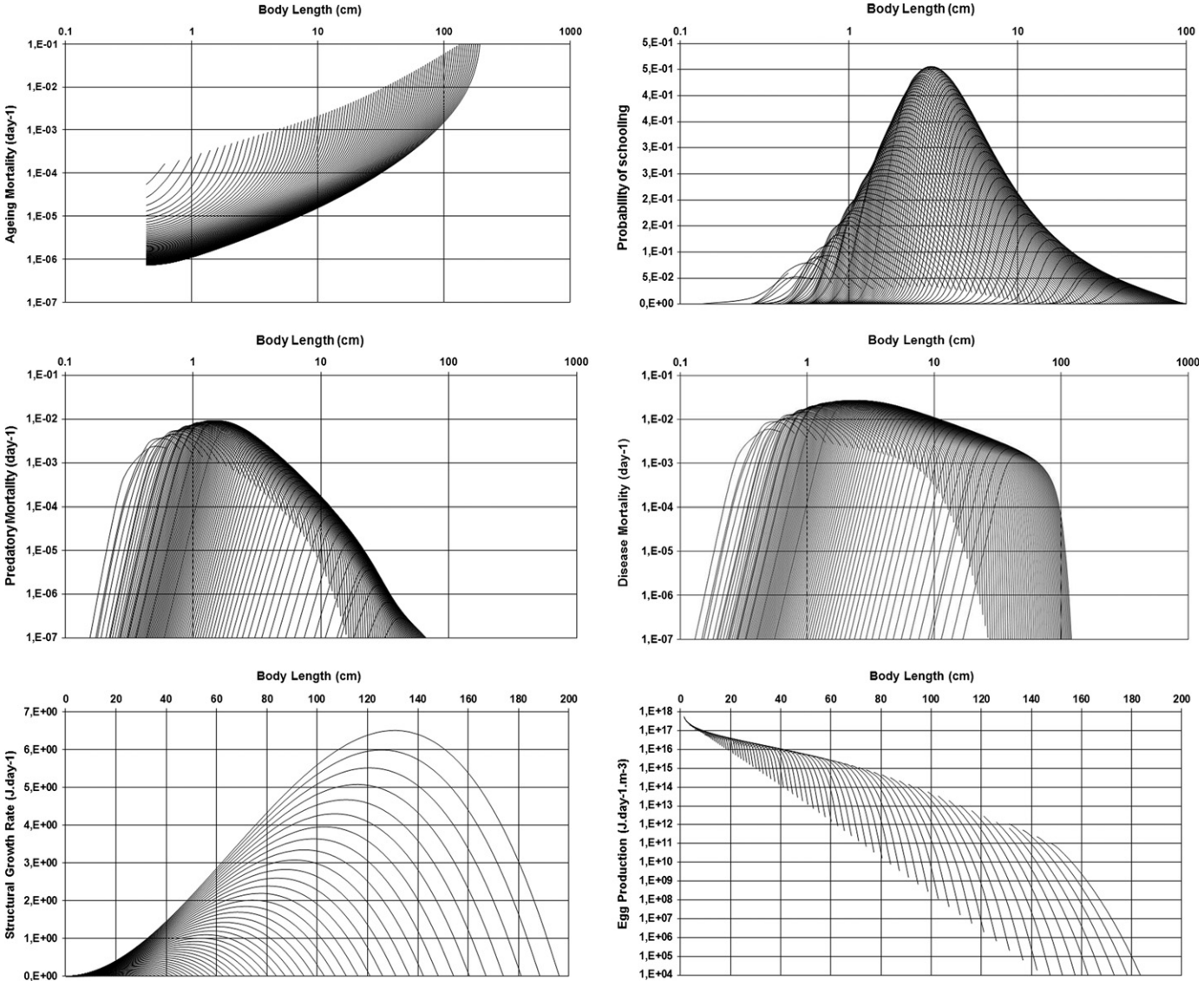

Fig. 5. Stationary solution of the model as a function of body length for all the species considered. From left to right and top to bottom: (a) ageing mortality; (b) probability of schooling (c) predatory mortality; (d) disease mortality; (e) structural growth rate; and (f) reproductive output.

rates as well as the structural growth rate and the reproductive output per size classes at steady state. At steady state, the log–log ageing mortality curve (Fig. 5a) exhibits a characteristic increasing shape which is the same for all species with low values at small sizes and larger values at large sizes. Compared to small species, large species have lower ageing mortalities at small sizes and higher at large sizes. The species-specific size-dependant probability of schooling (Fig. 5b) is dome shaped with maximum values above 0.5 occurring for sizes in the range 1.5–3 cm and species having maximum length in between 10 and 40 cm. The log–log predatory mortality curve at steady state (Fig. 5c) is dome shaped for individual species and exhibit high values for small species only. At the community level, the predation mortality is maximal at 1.5 cm and decreases sharply above. The disease mortality curves (Fig. 5d) are also dome shaped for individual species. They reach high values for medium to large size species, in a narrow range of size which increases with the ultimate size. The structural growth rate as a function of organism size is dome shaped for every species, reaching a maximum for intermediate to large sizes and then decreasing down to zero for length equal to L_∞ (Fig. 5e). The log–log contribution of each size class to egg production (R_t) at steady state (Fig. 5f) exhibit a decreasing trend with a downward curvature for sizes above 1.4 m. Large species reproduce at larger sizes and produce less egg than small species.

When the reference values of the parameters (Table 1) are used, the slope of the quasi-linear section of the stationary biomass length-spectrum equals -3.45 which is equivalent to a slope equal to -1.15 for the structural volume-spectrum (Fig. 6).

The stationary Φ function emerging from our simulation is provided Fig. 7. It represents the frequency distribution of species (maximal structural volume) for every size (structural volume) in the community. As such, it characterizes the structure of the community in term of the relative contribution of the various species. The Φ function is a dome-shaped function which equals

Fig. 6. Stationary body size spectrum for the 100 individual species considered (thin gray lines), the community (thick black line) and fitted power law (dashed line).

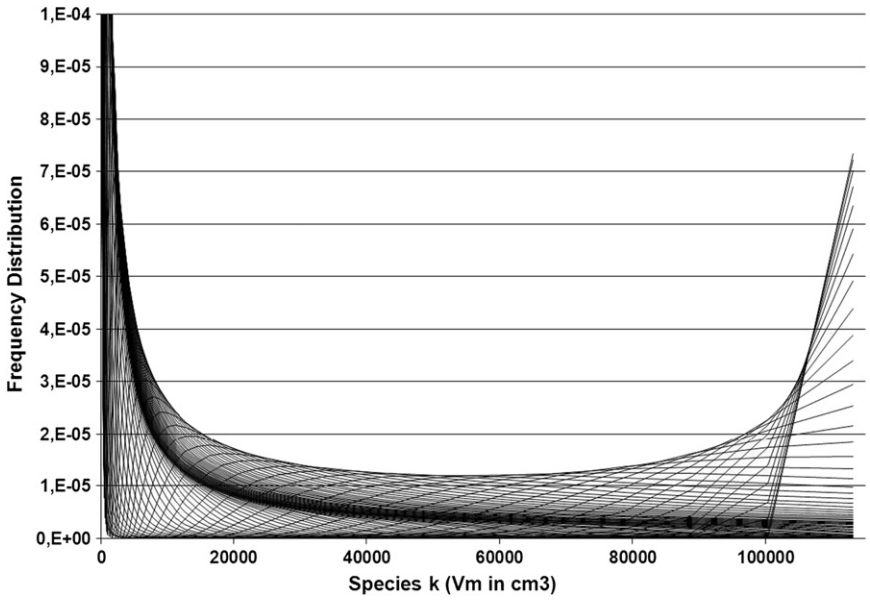

Fig. 7. StationaryΦ, functions. Each line represents, for a given structural volume, the frequency distribution of each species k.

zero for every species with a maximal structural volume smaller than the structural volume considered and with a long tail slowly decreasing to zero for large species. It is narrow for small sizes and more flattened and stretched for large sizes. The Φ function is truncated at the largest maximal structural volume considered.

Fig. 8 provides the total biomass (size integrated), the biomass of juveniles and the reproductive input (a) and the total biomass and eggs biomass per egg production (b) for every life history (maximal structural volume) considered. It shows that the total biomass, biomass of eggs and egg production are non-linearly decreasing with the size of the species considered (Fig. 8a). However, the total biomass by unit of egg produced is a decreasing function of the maximal size while the total biomass per egg production increases faster and faster with maximal size (Fig. 8b).

3.2. Non-stationary dynamics

Sinusoidal oscillations of the carrying capacity of producers have been simulated around the mean level considered previously, considering two characteristic periods: 1 year and 5 years. Those oscillations generate bumps propagating along the community size-spectrum while flattening when moving from

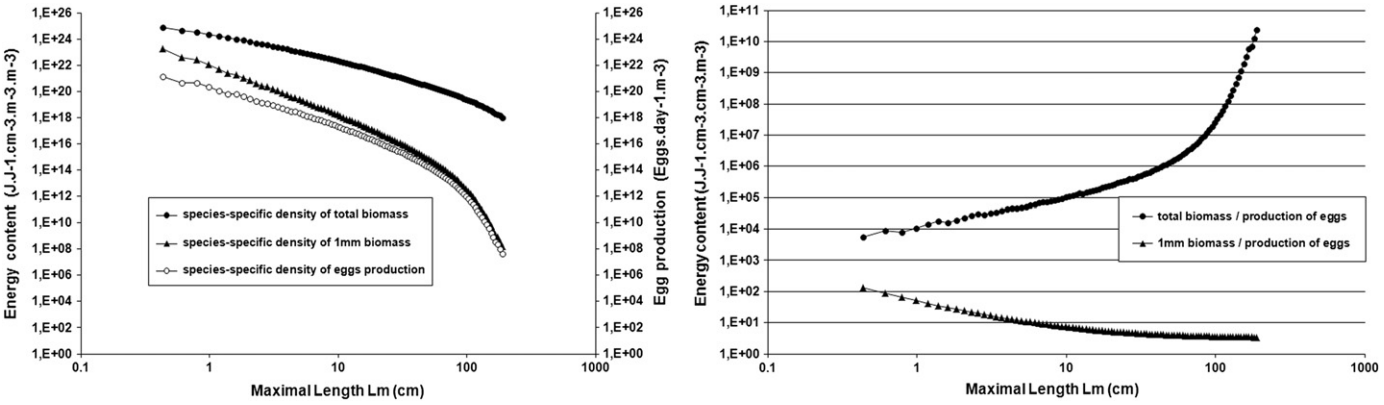

Fig. 8. (a) species-specific density of total biomass, 1 mm biomass and eggs production as a function of maximal length and (b) species-specific total biomass and 1 mm biomass relative to egg production

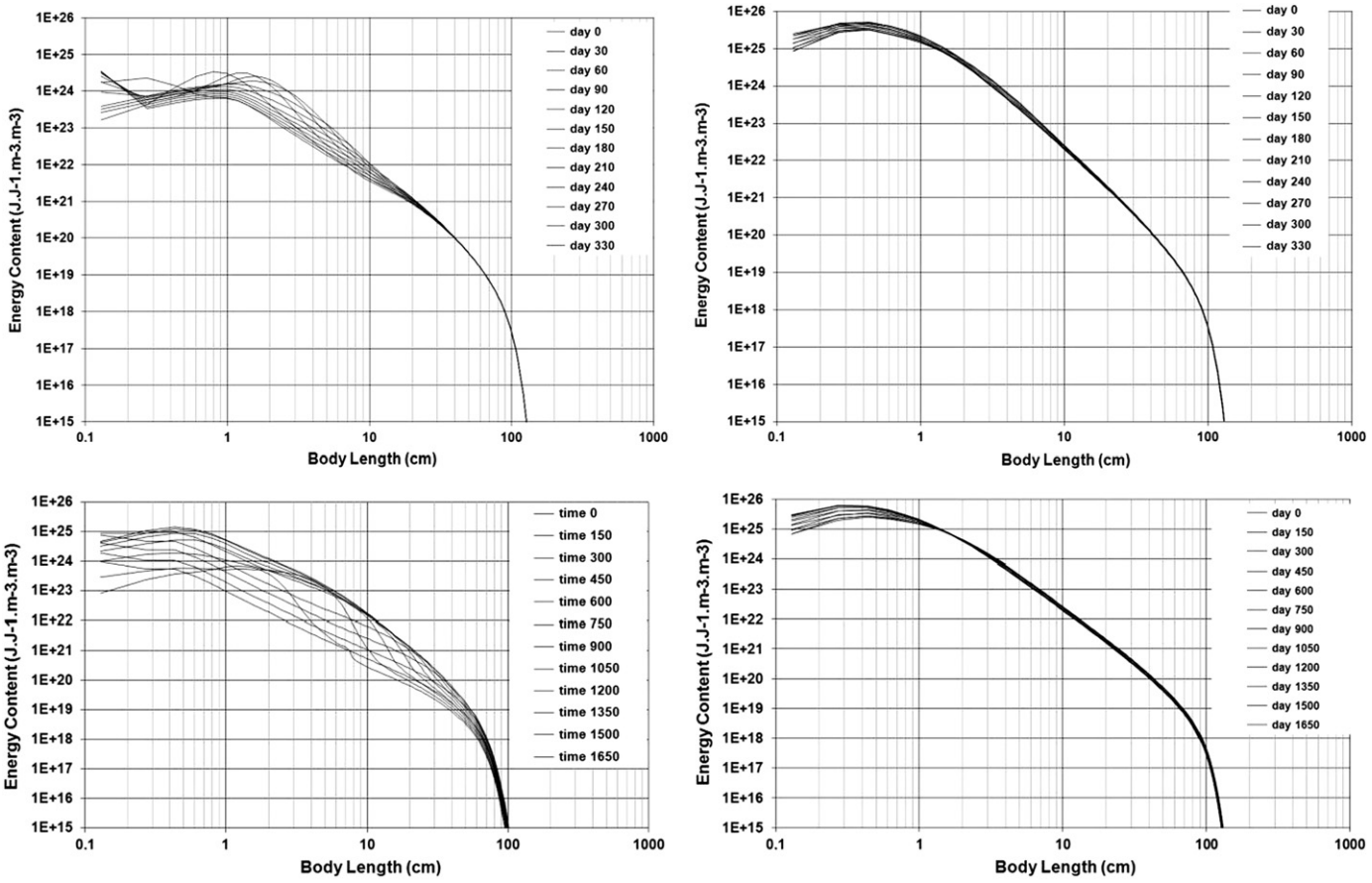

Fig. 9. Biomass size spectrum of the community in oscillatory environmental conditions. From left to right and top to bottom: (a) oscillation of producers with a 1 year period and 100% amplitude; (b) oscillation of temperature with a 1 year period and 10 °C amplitude; (c) oscillation of producers with a 5 year period and 100% amplitude; and (d) oscillation of temperature with a 5 year period and 10 °C amplitude.

small to large sizes (Fig. 9a and b). The variability of the community spectrum is maximal over a given range of size and then it declines until a critical size where the oscillations disappear and the spectrum is quasi-stationary. Both the range of variable sizes and the critical size above which there is no more variability depend on the periodicity of the oscillations of producers, the critical size being around 30 cm for yearly oscillations and 100 cm for 5 years oscillations.

4. Discussion

4.1. Linking individual metabolism, population dynamics and community diversity

The dynamics of marine communities emerges from complex interactions between individual metabolisms, food web processes and life history diversity in the community. Understanding the response of communities to environmental variability requires a framework which relates and integrates the various processes involved, at the individual, population and community levels. To our knowledge, our study constitutes the first attempt to derive mechanistically the dynamic size-spectrum of a diversified aquatic community including an infinitely large number of interacting species covering a broad range of life histories from the Dynamic Energy Budget of individual organisms. Our model is strictly based on the DEB theory. As such, it integrates mechanistically the following biological processes:

- surface-dependent food intake,
- distinction between reserve and structure,
- allocation of energy from reserves to growth and reproduction/development,
- volume-specific somatic and maturity maintenance,
- ageing mortality,
- starvation mortality,
- life history diversity through inter-specific scaling rules of maximum surface-specific assimilation rates, maximum reserve energy densities, structural volumes at puberty and birth, half saturation constants of the Holling functional response,
- temperature-dependence of physiological rates.

Furthermore, a set of important ecological processes are also integrated in the model:

- size-structured opportunistic trophic interactions where producers are potential prey and where all consumer species are potentially prey and predator simultaneously depending on the predator/prey size ratios (Jennings et al., 2001; Jennings et al., 2002; Shin and Cury, 2004; Maury et al., 2007a),
- predators competition for preys,

Finally, density-dependent processes are hypothesized to stabilize the model:

- density-dependent schooling probability,
- schooling-dependent availability of prey,
- schooling-dependent disease mortality.

We believe that accounting for those key biological and ecological processes simultaneously while keeping the functional complexity limited is a necessary step toward the development of the next generation of ecosystem models which will have to embody a high degree of mechanistic details, ecological realism, generality and theoretical consistency to ultimately achieve reliable predictive capabilities (Maury, 2010). Furthermore, all the biological and ecological processes considered are tight together and the model keeps a reasonable number of parameters. Besides, the strong mechanistic basis of the model and its individual level bases give a biological and ecological meaning to variables and parameters and hence allow for empirical testing and interpretation.

4.2. Unstable oscillations and the need for density-dependent feedbacks

In the absence of density-dependent regulation, the model exhibits unstable behavior with the propagation of traveling waves along the size dimension at both the species and community levels (not shown). This is not surprising since such unstable oscillations have been shown to be a likely behavior of simpler non-linear size-spectra models (Arino et al., 2004; Datta et al., 2011; Hartvig et al., 2011). From a biological point of view, those instabilities are linked to the existence of delayed feedbacks such as the "predator pit" effect (Bakun, 2006, 2009). Since small short-lived prey species have a shorter life cycle and hence vary more rapidly than larger long-lived predator species, any increase of their abundance results in a temporary decrease of the predatory mortality they undergo. Once a critical threshold is reached, the predatory mortality becomes negligible and the short lived prey species populations grow exponentially until the long-lived predator species have grown sufficiently to exert again a predatory control and lower the prey species abundance again. Then the opposite effect takes place and the predatory mortality that short lived prey species undergo increases suddenly as their abundance decreases (this is the "predator pit" in which prey populations fall) leading to the exhaustion of their populations. This "predator pit" effect is likely to generate oscillations which might be further enhanced by cultivation effect (Walters and Kitchell, 2001; Bakun and Weeks, 2006; Vergnon et al., 2009). The cultivation effect is due to the fact that prey species often consume the eggs and larvae of their predators thus exerting a control on their populations which might contribute to out of phase oscillations between predator and prey.

Though not necessarily unrealistic in highly variable systems such as upwelling systems, unstable oscillations are generally not observed in reality where strong density-dependent processes must be acting to explain the stability of community size spectra (e.g. Jennings, 2005). In the present study we propose that density-dependent schooling associated with schooling-dependent availability of prey and disease mortality could play a strong stabilizing role in marine ecosystems. Including those processes in our simulations indeed allows to stabilize the system and to obtain realistic and interpretable steady state solutions. However, schooling is likely not the only important density-dependent phenomenon affecting marine populations and other feedbacks are probably playing an important role in nature. Amongst those feedbacks, spatial effects are likely important. The ability of top predators to move quickly toward areas with higher prey density is indeed dramatically increasing their foraging efficiency which probably enhances their importance as regulatory factors (e.g. Moloney et al., 2010). As a matter of fact, top predators are large and mobile and they cover broad spatial ranges with potentially extensive movements and migrations to find the highest prey concentrations in the ocean (Fonteneau et al., 2008; Weimerskirch et al., 2004; Block et al., 2003). Because they occupy the highest position in food webs, top predators exert high predation levels (Bax, 1998; Essington et al., 2002) leading to a strong top-down control on their prey: they harvest the crests

and dampen the high frequency pulses and oscillations exhibited by lower levels (Moloney et al., 2010). Having wide distributional ranges and exhibiting extensive migrations, they also prey on different and asynchronous regional ecosystems potentially inshore and offshore (Young et al., 2001) or epipelagic and mesopelagic (Potier et al., 2007; Ménard et al., 2007). By preying on many different ecosystems, top predators have the ability to emancipate from local prey variations and they probably act as strong stabilizing factors, regulating the variability of lower levels and increasing the stability of the whole ecosystem (Moloney et al., 2010). The non-spatialized 0-D analysis presented here does not allow an explicit representation of those spatial processes. They should however not be underestimated and they should be included in future studies (Maury, 2010).

4.3. The density-dependence of schooling

In our model, schooling is used to obtain stable, non-oscillatory stationary solutions. We assume that aggregative behavior, which is a prominent feature of marine organisms, only leads to schooling when the density of size- and species-specific biomass is sufficient. Below this critical biomass density, schools are not sustainable and organisms are assumed to be dispersed. Schooling is the result of complex auto-organization phenomenon (Gautrais et al., 2008) and the existence of a clear density-dependent transition phase between dispersed and schooled fish distribution has been demonstrated both empirically (Becco et al., 2006) and theoretically (Vicsek et al., 1995; Czirok and Vicsek, 2000; Tu, 2000) and observed in the field (Makris et al., 2009). Given that the size-dependent density of biomass of a species depends on its ultimate length (Figs. 3 and 4) and that the critical biomass density at which schooling occurs is assumed to be a constant, the species-specific size-dependent probability of schooling is also dependent of maximum length (Fig. 5b). This corroborates the common observation that small individuals of small species most of the time form schools while small individuals of large species such as tunas remain dispersed and are extremely rarely observed (Fonteneau com. pers.). In the same perspective, Fréon and Misund (1999) report that northern anchovies (*Engraulis mordax*) (Lm$\sim$25 cm) acquire the physiological ability to school at 10–15 mm, Atlantic menhaden (*Brevoortia tyrannus*) (Lm$\sim$50 cm) at 22–25 mm and Atlantic herring (*Clupea harengus*) (Lm$\sim$45 cm) at 35–40 mm. Large fish such as skipjack tuna (*Katsuwonus pelamis*) (Lm$\sim$110 cm) or yellowfin tuna (*Thunnus albacares*) (Lm$\sim$180 cm) appear in commercial purse seine fisheries targeting free swimming schools respectively at 20 cm and 30 cm, thus indicating that below those sizes, tunas are mostly dispersed and escape predators and commercial purse-seiners (e.g. ICCAT, 2009). Our simulation results provide a consistent explanation for those various heterogeneous observations. They furthermore show that species with a maximum size around 10 cm reach the highest probabilities of schooling while very large and very small species never reach high probabilities of schooling (Fig. 5b).

4.4. Stationary solutions

When the carrying capacity of producers is kept constant, the model converges toward a stationary size-spectrum independent of initial conditions and quasi-linear in log–log with a slope -3.5 within a wide range of sizes (Fig. 6). This stationary solution is obtained when the transport of individuals (in and out of each size class) is exactly balanced by mortality. This corroborates the results of previous theoretical studies showing that size-structured predator–prey models admit a linear log–log size-spectrum as a stationary solution (Silvert and Platt, 1980; Arino et al., 2004; Benoit and Rochet, 2004; Maury et al., 2007a) as far as the smallest and largest sizes are put apart (Shin and Cury, 2004; Maury et al., 2007a). Furthermore, using our reference set of parameters (Table 2), the slope of the quasi-linear section of the spectrum matches fairly well the values reported in empirical studies (e.g. MacPherson and Gordoa, 1996; Zhou and Huntley, 1997; Quiñones et al., 2003; Marquet et al., 2005). For the small size classes of the fish community spectrum, the model departs from the linear solution and is markedly curved. If smaller communities of consumers such as copepods for instance were considered in the analysis, their community size-spectrum would likely fill the gap for small sizes, leading to a quasi-linear spectrum at the scale of the ecosystem i.e. including small and large communities.

The log–log spectrum also departs from the linear solution for the largest sizes, where only the largest species remain and where their biomass is substantially influenced by ageing mortality which is no longer negligible (Fig. 5a). This curvature of the community spectrum would be translated to larger sizes if larger species were considered in the simulation (the largest species considered here has a maximal body length of 2 m only). Furthermore, Kooijman (2010) and Van Leeuwen et al. (2010) improved the representation of ageing in the DEB theory allowing for more flexibility of the ageing acceleration. Including this new formulation in our model would increase the suddenness of the increase of ageing mortality, thus modifying the curvature of the community spectrum by increasing its steepness and shifting its occurrence toward larger sizes. This would also increase the time during which large species reproduce and hence increase (less negative) the slope of the community spectrum by increasing the abundance of large species.

In term of species-specific size distribution, the stationary solution of the model, whether expressed in number or in biomass (Figs. 3 and 4), clearly shows that small and large species dominate the community successively, small species being more abundant than large ones at small sizes and large species being more abundant at large sizes. This has to be related to their different life histories: large species have higher reproduction rates than small ones (Kooijman, 2000) but they reach puberty at such a larger size (proportional to their maximal length) that despite their higher growth rate (Fig. 5e), they reproduce much later that small species and hence have a much longer generation time. The dependence of generation time on maximum size explains that small species produce more eggs and are more abundant than large one (Fig. 5f). Furthermore, our results predict that the stationary species-specific total biomass decreases with the maximal size of the species considered (Fig. 8a). This corroborates empirical observations (Blueweiss et al., 1978; Marquet et al., 2005; Woodward et al., 2005; White et al., 2007) as well as theoretical studies (Andersen and Beyer, 2006) which show that the abundance of natural fish populations decreases with the maximal size of the considered species. It should also be noted that the biomass of eggs decreases faster than the total biomass with the size of the species considered (Fig. 8a) and that the total biomass per egg production increases with the size of the species considered (Fig. 8b), demonstrating that large species are "storing" biomass more efficiently than small ones.

4.5. Non-stationary solutions

When oscillations of primary production are simulated, the model predicts that the variability propagates along the spectrum (Fig. 9a and c) in a given size range before decreasing for larger sizes. The size range corresponding to the maximum amplitude of the relative energy density, that we call the "resonant range", is frequency dependent, it depends on the period of the primary

production oscillations. High frequency oscillations of primary production lead to a "resonant range" limited to small sizes whereas low frequency oscillations lead to a "resonant range" also reaching larger sizes.

Small species feed on producers or on very close size ranges. They furthermore grow and die very quickly (their characteristic time – the time needed to reach the size of puberty – is shorter than the period of phytoplankton oscillations – 1 year-) so that they can adapt very rapidly to changes and track primary production variability. In consequence, they oscillate more or less in phase with producers (Fig. 9a): they are bottom-up controlled by primary production oscillations. When the maximum body size increases, the characteristic time also increases. When the characteristic time exceeds the period of phytoplankton oscillations, the system leaves the "resonant range". Furthermore, organisms larger than the "resonant range" can feed on a wide range of prey size covering several out of phase oscillations. They are emancipated from the temporary disappearance of a certain size range of their prey since they can compensate by reporting their predation effort on abundant size classes: they are not influenced by bottom-up effects of phytoplankton high frequency oscillations.

Oscillations of the size spectrum have been reported by various authors (Jiménez et al., 1989; Edvardsen et al., 2002; Fossheim et al., 2005). For instance, Fossheim et al. (2005, Figure 5) observed oscillations for small sizes (up to 1 mm) of zooplankton size spectrum recorded with an Optical Plankton Counter (OPC). Given their frequency and the very fast growth rate of zooplankton, those oscillations could be linked to nyctimeral oscillations of the zooplankton feeding activity.

4.6. Is the Φ function a measure of functional diversity at the community level?

When attempting to aggregate the full species-based model into a model of the community size-spectrum which does not include an explicit representation of the species level (see Section 2.4), an undetermined function $\Phi^k_{t,V}$ appears in the calculations. The function $\Phi^k_{t,V}$ is an emergent property of the system considered. It expresses the relative contribution of each species k to the total energy content (biomass) of the ecosystem, for any given structural volume V. When the system is in a stationary state, $\Phi^k_{t,V}$ is also stationary (Fig. 7) and clearly shows that the range of species contributing most to the biomass of a size class changes dramatically with the size class considered. The function $\Phi^k_{t,V}$ admits a maximum with respect to the maximal volume. At a given structural volume, the most abundant species belong to a range of maximal sizes which translates toward large species (more large species and less small species) when the structural volume considered increases. Given that small and large species do not have the same metabolic parameters, the function $\Phi^k_{t,V}$ characterizes the speed and dispersion of energy flow along the size dimension and the relative proportions of losses (mortalities), dissipation (maintenance and other dissipative processes of the metabolism) and biological work (growth and reproduction) at the community level. Any change of the function $\Phi^k_{t,V}$ implies changes of those emergent metabolic properties at the community level. Consequently, the $\Phi^k_{t,V}$ function can be considered as a measure of the functional role of biodiversity characterizing the impact of the structure of the community (its species composition) on its function (the various energy fluxes).

The $\Phi^k_{t,V}$ function is unknown but it could be approached either using parametric or non-parametric (such as B-splines) approximations fitted to numerical simulations using the full species-based model. This is straightforward when the system is in a steady state. However, when it is not, in the case of environmental fluctuations for instance, the $\Phi^k_{t,V}$ function becomes time-dependent (not shown), expressing the fact that small species are quicker to adapt to environmental changes than large species. In this non-stationary case, the behavior of the $\Phi^k_{t,V}$ function would need to be studied in more details. This would include further theoretical and numerical studies as well as empirical studies in the field.

5. Conclusion

In this paper we attempt to link the bio-energetic and life history of species-specific individuals to the size-structured dynamics of their populations and the dynamics of their community which includes an infinite number of interacting populations. The numerical results presented here indicate that the simultaneous consideration of individual growth and reproduction, size-structured trophic interactions, the diversity of life-history traits and a density-dependent stabilizing process allow realistic community structure and dynamics to emerge without any arbitrary prescription. Dealing explicitly with all the possible species in a community would not be possible without the generality of the DEB theory which captures the diversity of all the possible living forms on earth in a single mechanistic framework (Kooijman, 2010; Sousa et al., 2010). It furthermore explains the interspecific scaling relationships of life history parameters which are commonly observed in nature and demonstrates that they are due to the fact that some DEB parameters are constant amongst species while some others are proportional to the maximum volumetric length of the species considered. This allows representing the energetic and major life history traits of all possible species in a community with the same set of unspecific taxa-dependent DEB parameters. The existence of such scaling parameters which are independent of the species considered is a fundamental property of the DEB theory. They emphasize the fundamental importance of the size of the species and imply that functional (in terms of energetic and life history) biodiversity has actually far less degrees of freedom that one would expect given the high number of possible species. This major finding might open the way to a mechanistic understanding of biodiversity and ecosystems dynamics. The present paper attempts to walk a step in that direction.

Acknowledgments

The authors would like to thank Bas Kooijman, Tania Sousa and Tiago Domingos for their comments on an earlier version of this paper. We also would like to thank Sibylle Dueri for her help in drawing nicely one of the figures. Both authors acknowledge the support of the French ANR, under the grant CEP MACROES (MACRoscope for Oceanic Earth System ANR-09-CEP-003). This work is a contribution to the CLIOTOP Synthesis and Modeling Working Group.

Appendix A. Model reduction

Quantities characteristic of the processes considered are used to adimensionalize the model. Through this classical process, fast and slow dynamics appear. They are characterized by a small parameter ε. We then derive a reduced model passing to the limit $\varepsilon=0$.

The full model is given by Eq. (5.) which is rewritten below for convenience:

$$\begin{cases} \partial_t N^k_{t,E,V} = -\partial_V(\gamma^k_{t,E,V} N^k_{t,E,V}) - \partial_E(\eta^k_{t,E,V} N^k_{t,E,V}) \\ \qquad -(\lambda^k_{t,E,V} + a^k_{t,E,V} + s^k_{t,E,V} + z^k_{t,E,V}) N^k_{t,E,V} \\ N^k_{0,E,V} = N^{k,0}_{E,V} \\ \gamma^k_{t,E,V_b} N^k_{t,E,V_b} = r^k_{t,E} \end{cases} \tag{A1}$$

In what follows the letter S refers to characteristic scales (for instance S_V for the structural volume scale). For a variable with dimension, e.g. V, the notation $\tilde{V}$ refers to the adimensionalized variable.

Let us define the characteristic scales $V = S_V\tilde{V}$ in the structural volume dimension, $E = S_E\tilde{E}$ in the reserve dimension, $k = S_k\tilde{k}$ in the species dimension and $t = S_t\tilde{t}$ for time. Let us also define for the density of population abundance N a new adimentionalized state variable so that

$$N(V,E,t) = S_N\tilde{N}(\tilde{V},\tilde{E},\tilde{t}) \tag{A2}$$

All the processes involved in the dynamic of the system are also adimentionalized as follows:

- *Structural growth*:
$$\dot{\gamma} = S_\gamma\tilde{\gamma} \tag{A3}$$
- Reserve dynamics:
$$\dot{\eta} = S_\eta\tilde{\eta} \tag{A4}$$
- Mortality:
$$\dot{\lambda} + \dot{a} + \dot{s} + \dot{z} = S_M(\tilde{\lambda} + \tilde{a} + \tilde{s} + \tilde{z}) \tag{A5}$$
- Newborn input:
$$\dot{r} = S_R\tilde{r} \tag{A6}$$

The density function $\tilde{N}^{\tilde{k}}_{\tilde{t},\tilde{E},\tilde{V}}$ follows:

$$\begin{cases} \partial_{\tilde{t}}\tilde{N}^{\tilde{k}}_{\tilde{t},\tilde{E},\tilde{V}} = -\frac{S_tS_\gamma}{S_V}(\tilde{\gamma}\tilde{N}^{\tilde{k}}_{\tilde{t},\tilde{E},\tilde{V}}) - \frac{S_tS_\eta}{S_E}\partial_{\tilde{E}}(\tilde{\eta}\tilde{N}^{\tilde{k}}_{\tilde{t},\tilde{E},\tilde{V}}) \\ \quad -S_tS_M\left(\tilde{\lambda}^{\tilde{k}}_{\tilde{t},\tilde{E},\tilde{V}} + \tilde{a}^{\tilde{k}}_{\tilde{t},\tilde{E},\tilde{V}} + \tilde{s}^{\tilde{k}}_{\tilde{t},\tilde{E},\tilde{V}} + \tilde{z}^{\tilde{k}}_{\tilde{t},\tilde{E},\tilde{V}}\right) \\ \tilde{N}^{\tilde{k}}_{\tilde{t},\tilde{E},\tilde{V}}\tilde{N}^{\tilde{k}}_{0,\tilde{E},\tilde{V}} = \tilde{N}^{\tilde{k},0}_{\tilde{E},\tilde{V}} \end{cases} \tag{A7}$$

To introduce scale differences in the characteristic dimensions, let us define a small parameter $|\varepsilon| \ll 1$ and assume that

$$\frac{S_\gamma/S_V}{S_\eta/S_E} = \varepsilon \tag{A8}$$

$$S_t = \frac{S_V}{S_\gamma} \tag{A9}$$

$$S_tS_M = \varepsilon \tag{A10}$$

$$\frac{S_R}{S_\eta} = \varepsilon \tag{A11}$$

Using those assumptions, Eq. (A7) can be rewritten as follows:

$$\begin{aligned} \partial_{\tilde{t}}\tilde{N}^{\tilde{k}}_{\tilde{t},\tilde{E},\tilde{V}} = &-\partial_{\tilde{V}}(\tilde{\gamma}\tilde{N}^{\tilde{k}}_{\tilde{t},\tilde{E},\tilde{V}}) - \frac{1}{\varepsilon}\partial_{\tilde{E}}(\tilde{\eta}\tilde{N}^{\tilde{k}}_{\tilde{t},\tilde{E},\tilde{V}}) \\ &-\varepsilon\left(\tilde{\lambda}^{\tilde{k}}_{\tilde{t},\tilde{E},\tilde{V}} + \tilde{a}^{\tilde{k}}_{\tilde{t},\tilde{E},\tilde{V}} + \tilde{s}^{\tilde{k}}_{\tilde{t},\tilde{E},\tilde{V}} + \tilde{z}^{\tilde{k}}_{\tilde{t},\tilde{E},\tilde{V}}\right)\tilde{N}^{\tilde{k}}_{\tilde{t},\tilde{E},\tilde{V}} \end{aligned} \tag{A12}$$

Multiplying both sides of Eq. (A12) by ε and taking $\varepsilon = 0$ leads to

$$\partial_{\tilde{E}}(\tilde{\eta}\tilde{N}^{\tilde{k}}_{\tilde{t},\tilde{E},\tilde{V}}) = 0 \tag{A13}$$

which is equivalent to

$$\tilde{\eta}\tilde{N}^{\tilde{k}}_{\tilde{t},\tilde{E},\tilde{V}} = c_{\tilde{t},\tilde{V}} \tag{A14}$$

with c a constant independent of $\tilde{E}$

$$\begin{aligned} &\dot{\eta} = V\frac{d[E]}{dt} + \frac{E}{V}\frac{dV}{dt} \\ &\Rightarrow \tilde{\eta} = \frac{S_E}{S_V}\frac{S_\gamma}{S_\eta}\tilde{V}\frac{d[\tilde{E}]}{d\tilde{t}} + \frac{S_E}{S_V}\frac{S_\gamma}{S_\eta}\frac{\tilde{E}}{\tilde{V}}\frac{d\tilde{V}}{d\tilde{t}} = \varepsilon\left(\tilde{V}\frac{d[\tilde{E}]}{d\tilde{t}} + \frac{\tilde{E}}{\tilde{V}}\frac{d\tilde{V}}{d\tilde{t}}\right) \end{aligned} \tag{A15}$$

Taking $\varepsilon = 0$ leads to $\tilde{\eta} = 0$ so that $c = 0$.

Since $\tilde{\eta}$ is always strictly positive except when $\tilde{E} = \tilde{E}^*$ and $\int_{\tilde{E}=0}^{\tilde{E}_m}\tilde{N}^{\tilde{k}}_{\tilde{t},\tilde{E},\tilde{V}}d\tilde{E} > 0$, Eq. (A14) implies that $\tilde{N}^{\tilde{k}}_{\tilde{t},\tilde{E},\tilde{V}}$ is always null except for $\tilde{E} = \tilde{E}^*$ so that the density function $\tilde{N}^{\tilde{k}}_{\tilde{t},\tilde{E},\tilde{V}}$ is proportional to a dirac function in $\tilde{E}^*$

$$\tilde{N}^{\tilde{k}}_{\tilde{t},\tilde{E},\tilde{V}} = \delta(\tilde{E} - \tilde{E}^*)\int_{\tilde{E}=0}^{\tilde{E}_m}\tilde{N}^{\tilde{k}}_{\tilde{t},\tilde{E},\tilde{V}}d\tilde{E} \tag{A16}$$

Let us now define the new state variable of the reduced model by integrating Eq. (A7.) on $(0,\tilde{E}_m)$

$$\overline{N}_{\tilde{t},\tilde{V}} = \int_0^{\tilde{E}_m}\tilde{N}^{\tilde{k}}_{\tilde{t},\tilde{E},\tilde{V}}d\tilde{E} \tag{A17}$$

Let us also define the average of any variable along the reserve profile as

$$\overline{g} = \frac{\int_0^{\tilde{E}_m}\tilde{g}(\tilde{E})\delta(\tilde{E} - \tilde{E}^*)d\tilde{E}}{\int_0^{\tilde{E}_m}\delta(\tilde{E} - \tilde{E}^*)d\tilde{E}} = \tilde{g}(\tilde{E}^*) \tag{A18}$$

Using this notation, we integrate Eq. (A7) over $(0,\tilde{E}_m)$ in order to derive an equation of evolution for $\overline{N}$

- Time derivative term:
$$\int_0^{\tilde{E}_m}\partial_{\tilde{t}}\tilde{N}^{\tilde{k}}_{\tilde{t},\tilde{E},\tilde{V}}d\tilde{E} = \partial_{\tilde{t}}\overline{N}^{\tilde{k}}_{\tilde{t},\tilde{V}} \tag{A19}$$
- Structural growth terms:
$$\int_0^{\tilde{E}_m}\partial_{\tilde{V}}(\tilde{\gamma}\tilde{N}^{\tilde{k}}_{\tilde{t},\tilde{E},\tilde{V}})d\tilde{E} = \partial_{\tilde{V}}(\overline{\gamma}\overline{N}^{\tilde{k}}_{\tilde{t},\tilde{V}}) \tag{A20}$$
- Mortality terms:
$$\begin{aligned} &\int_0^{\tilde{E}_m}\left(\tilde{\lambda}^{\tilde{k}}_{\tilde{t},\tilde{E},\tilde{V}} + \tilde{a}^{\tilde{k}}_{\tilde{t},\tilde{E},\tilde{V}} + \tilde{s}^{\tilde{k}}_{\tilde{t},\tilde{E},\tilde{V}} + \tilde{z}^{\tilde{k}}_{\tilde{t},\tilde{E},\tilde{V}}\right)\tilde{N}^{\tilde{k}}_{\tilde{t},\tilde{E},\tilde{V}}d\tilde{E} \\ &\quad = \left(\overline{\lambda}^{\tilde{k}}_{\tilde{t},\tilde{V}} + \overline{a}^{\tilde{k}}_{\tilde{t},\tilde{V}} + \overline{s}^{\tilde{k}}_{\tilde{t},\tilde{V}} + \overline{z}^{\tilde{k}}_{\tilde{t},\tilde{V}}\right)\overline{N}^{\tilde{k}}_{\tilde{t},\tilde{V}} \end{aligned} \tag{A21}$$
- Recruitment term:
$$\int_0^{\tilde{E}_m}\tilde{\gamma}_{\tilde{V}_b}\tilde{N}^{\tilde{k}}_{\tilde{t},\tilde{E},\tilde{V}_b}d\tilde{E} = \overline{\gamma}_{\tilde{V}}\overline{N}^{\tilde{k}}_{\tilde{t},\tilde{V}_b} \tag{A22}$$
- Thanks to the Neuman boundary condition on $\tilde{E}$ and to the scaling assumptions, the advection term in E vanishes.

The reduced model for the new state variable $\overline{N}$ finally reads

$$\begin{cases} \partial_{\tilde{t}}\overline{N}^{\tilde{k}}_{\tilde{t},\tilde{V}} = -\partial_{\tilde{V}}\left(\overline{\dot{\gamma}}_V \overline{N}^{\tilde{k}}_{\tilde{t},\tilde{V}}\right) - \varepsilon\left(\overline{\dot{\lambda}}^{\tilde{k}}_{\tilde{t},\tilde{V}} + \overline{\dot{a}}^{\tilde{k}}_{\tilde{t},\tilde{V}} + \overline{\dot{s}}^{\tilde{k}}_{\tilde{t},\tilde{V}} + \overline{\dot{z}}^{\tilde{k}}_{\tilde{t},\tilde{V}}\right)\overline{N}^{\tilde{k}}_{\tilde{t},\tilde{V}} \\ \overline{N}^{\tilde{k}}_{0,\tilde{V}} = \overline{N}^{\tilde{k},0}_{\tilde{V}} \\ \overline{\dot{\gamma}}_{\tilde{V}_b}\overline{N}^{\tilde{k}}_{t,\tilde{V}_b} = \varepsilon r(\overline{N}\tilde{k}) \end{cases} \tag{A23}$$

which is easily put back into dimensional form and results in the following model:

$$\begin{cases} \partial_t N^k_{t,E^*,V} = -\partial_V\left(\dot{\gamma} N^k_{t,E^*,V}\right) - \left(\dot{\lambda}^{\,k}_{t,E^*,V} + \dot{a}^k_{t,E^*,V} + \dot{s}^k_{t,E^*,V} + \dot{z}^k_{t,E^*,V}\right) N^k_{t,E^*,V} \\ N^k_{0,E^*,V} = N^{k,0}_{E^*,V} \\ \dot{\gamma}_{V_b} N^k_{t,E^*,V_b} = \dot{r}\left(N^k\right) \end{cases} \tag{A24}$$

Appendix B. Validity of scaling assumptions

We have to verify that $\frac{S_\gamma/S_V}{S_\eta/S_E} = \varepsilon$ with $|\varepsilon| \ll 1$ is an acceptable assumption. For that purpose, let us define the characteristic dimensions for energy in the reserve compartment and for structural volume as the maximum value that they can possibly take:

$$\begin{cases} S_E = [E_m]V_m \\ S_V = V_m \end{cases} \tag{B1}$$

Let us now define S_γ as the maximum growth rate that a given species can experiment as a function of f and e. Simple calculations show that $\dot{\gamma}$ is maximized for

$$V_{\max\dot{\gamma}} = \left(\frac{2\kappa\{\dot{p}_{A_m}\}e}{3[\dot{p}_M]}\right)^3 \tag{B2}$$

so that:

$$S_\gamma = \frac{\kappa\dot{v}[E_m]eV^{1/3}_{\max\dot{\gamma}} - [\dot{p}_M]V_{\max\dot{\gamma}}}{\kappa[E_m]e + [E_G]} = \frac{\kappa\alpha_{[\dot{p}_{Am}]}V_m^{1/3}eV^{1/3}_{\max\dot{\gamma}} - [\dot{p}_M]V_{\max\dot{\gamma}}}{\kappa\alpha_{[E_m]}V_m^{1/3}e + [E_G]} \tag{B3}$$

Let us now define S_η as the rate of reserve change $\dot{\eta}$ at $V = V_m$. It holds that

$$\dot{\eta} = \frac{dE}{dt} = V\frac{d[E]}{dt} + \frac{E}{V}\frac{dV}{dt} \tag{B4}$$

so that at $V = V_m$ we have

$$S_\eta = V_m\frac{d[E]}{dt} = V_m^{1/3}\{\dot{p}_{Am}\}(f-e) = V_m\alpha_{\{\dot{p}_{Am}\}}(f-e) \tag{B5}$$

Given Eqs. (B1), (B3) and (B5), we can express the ratio

$$\frac{S_\gamma/S_V}{S_\eta/S_E} = \frac{[E_m]}{V_m\alpha_{\{\dot{p}_{Am}\}}(f-e)}\left(\frac{\kappa\dot{v}\alpha_{[E_m]}V_m^{-2/3}eV^{1/3}_{\max\gamma_V} - [\dot{p}_M]V_m^{-1}V_{\max\gamma_V}}{\kappa\alpha_{[E_m]}V_m^{1/3}e + [E_G]}\right) \tag{B6}$$

and calculate it for various values of e and f (Fig. B1).

Given the scaling assumptions made and the orders of magnitude chosen for the characteristic dimensions, it is clear from (Fig. B1) that $|\varepsilon| \ll 1$ (i.e. $|\varepsilon| < 0.1$) is not always verified (except when $f=0$). However, $|\varepsilon| < 0.1$ is verified over a substantial domain when organisms are far from equilibrium ($e \ll f$ or $e \gg f$). Conversely, when organisms are close to equilibrium (i.e. when $e \approx f$), the assumption $|\varepsilon| \ll 0.1$ is no more verified but this is not problematic since the reserve compartment is already close to equilibrium where the density function $\tilde{N}_{\tilde{t},\tilde{E},\tilde{V}}$ is proportional to a dirac function in $\tilde{E}^*$ (cf. Eq. (A16)). The problematic domain is the intermediate one, when the reserve compartment of organisms is neither close to equilibrium, neither far from it. It this case, the

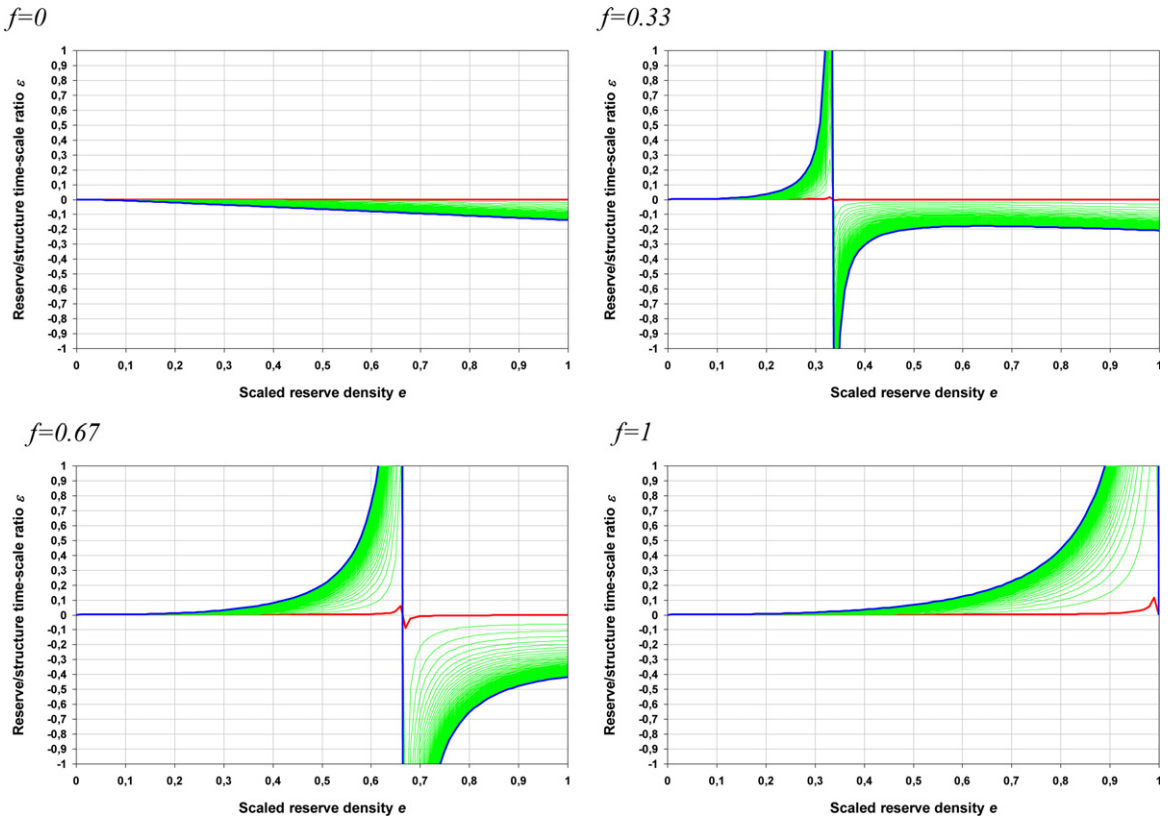

Fig. B1. $\varepsilon = (S_\gamma/S_V)/(S_\eta/S_E)$ is plotted as a function of the scaled energy density in the reserves e for 100 different species characterized by their Lm value ranging from 0.025 cm (red line),]0.025 cm, 50 cm[(green lines) to 50 cm (blue line) (with the shape parameter $\delta = 0.25$, this allows to cover a range of sizes $0.1\text{ cm} < L_\infty < 200\text{ cm}$). (For interpretation of the references to color in this figure legend, the reader is referred to the web version of this article.)

slow/fast approximation proposed might not be valid, especially for larger organisms. It has to be noted that since the reserve compartment spontaneously tends to equilibrium and hence tends to get out of the problematic domain, the mis-approximation is only transitory. This makes the problem related to the frequency (and amplitude) of environmental variability. Further work would be needed to study this problem in detail and compare the behavior of the full and the reduce model in different environmental variability conditions. This goes far beyond the present study.

Appendix C. From numbers to energy

Eq. (6) can be expressed in term of energy using $N^k_{t,E,V} = \xi^k_{t,E,V}/(E+d\psi V)$:

$$\begin{cases} \frac{\partial \frac{\xi^k_{t,E,V}}{E+d\psi V}}{\partial t} = -\frac{\partial\left(\dot\gamma^k_{t,V}\frac{\xi^k_{t,E,V}}{E+d\psi V}\right)}{\partial V} - \left(\dot\lambda^k_{t,E,V}+\dot a^k_{t,E,V}+\dot s^k_{t,E,V}+\dot z^k_{t,E,V}\right)\frac{\xi^k_{t,E,V}}{E+d\psi V} \\ \xi^k_{0,E,V} = \xi^{k,0}_{E,V} \end{cases} \tag{C1}$$

Simple calculations lead to

$$\frac{\partial \xi^k_{t,V}}{\partial t} = -\frac{\partial\left(\dot\gamma^k_{t,V}\xi^k_{t,V}\right)}{\partial V} + \frac{\gamma^k_{t,V}\xi^k_{t,V}}{d\psi V+E}\left(d\psi+\frac{\partial E}{\partial V}\right) - \left(\lambda^k_{t,V}+a^k_{t,V}+s^k_{t,V}+z^k_{t,V}\right)\xi^k_{t,V} \tag{C2}$$

Appendix D. Parameterizations of population rates

The predation process: calculation of $\lambda^k_{t,V}$

The function $s_{u,w}$ is a normalized function expressed as the product of two sigmoid functions which account for the limitation of ingestion when preys are either too small or too large (Maury et al., 2007a):

$$s_{u,w} = \left(1+e^{\alpha_1\left(\rho_1-\left(\frac{u}{w}\right)^{1/3}\right)}\right)^{-1}\left(1-\left(1+e^{\alpha_2\left(\rho_2-\left(\frac{u}{w}\right)^{1/3}\right)}\right)^{-1}\right)$$

$$\mathrm{R}^{+*2} \xrightarrow{s}]0;1[\tag{D1}$$

with ρ_1, ρ_2, α_1 and α_2, being constant positive parameters characterizing both the half saturation and the flatness of the sigmoid functions.

To calculate the predatory mortality, the amount of preyed energy $\mathrm{E}^{k/q}_{t,u/w} dk\,du\,dq\,dw\,dt$ (J m^{-3}) that predators of species $[k, k+dk]$ in the range of structural volume $[u, u+du]$ take from prey of species $[q, q+dq]$ in the range of structural volume $[w, w+dw]$ at time t during dt is expressed as follows, based on Eq. (11):

$$\begin{aligned} \mathrm{E}^{k/q}_{t,u/w}\ dk\ du\ dq\ dw\ dt &= \mathrm{E}^k_{t,u}\ dk\ du\ dt\frac{s_{u,w}ps^q_{t,w}\xi^q_{t,w}\ dq\ dw}{p_{t,u}} \\ &= \frac{\{\dot p^k_{Am}\}}{\kappa_X}\xi^k_{t,u}u^{-1/3}\frac{f^k_{t,u}}{d\psi+f^k_{t,u}[E^k_m]}\frac{s_{u,w}ps^q_{t,w}\xi^q_{t,w}dw}{p_{t,u}}\ dk\ du\ dq\ dt \\ &= \frac{\{\dot p^k_{Am}\}}{\kappa_X}\xi^k_{t,u}u^{-1/3}\frac{s_{u,w}ps^q_{t,w}\xi^q_{t,w}dw}{\dot c^k d\psi/u^\chi+(d\psi+[E^k_m])p_{t,u}}\ dk\ du\ dq\ dt \end{aligned} \tag{D2}$$

In the same way, the amount of preyed energy $\mathrm{E}^{k/p}_{t,u/w} dk\,du\,dw\,dt$ (J m^{-3}) that predators of species $[k, k+dk]$ in the range of structural volume $[u, u+du]$ take from producer organisms in the range of structural volume $[w, w+dw]$ at time t during dt is expressed as follows:

$$\mathrm{E}^{k/p}_{t,u/w}\ dk\ du\ dw\ dt = \frac{\left\{\dot p^k_{Am}\right\}}{\kappa_X}\xi^k_{t,u}u^{-1/3}\frac{s_{u,w}\widehat{\xi}^p_{t,w}dw}{\dot c^k d\psi/u^\chi+(d\psi+[E^k_m])p_{t,u}}\ dk\ du\ dt \tag{D3}$$

Given those equations, the total amount of energy preyed by all predators on all preys of species [q, q+dq] in the range of structural volume [w, w+dw] at time t during dt in 1 m^3 of water is then calculated by integration:

$$\begin{aligned} \mathrm{E}^{/q}_{t,/w}\ dq\ dw\ dt &= \int_{k=V_b}^{V^{k\max}_m}\int_{u=V_b}^{k}\mathrm{E}^{k/q}_{t,u/w}du\ dk\ dq\ dw\ dt \\ &= \frac{ps^q_{t,w}\xi^q_{t,w}}{\kappa_X}\int_{k=V_b}^{V^{k\max}_m}\int_{u=V_b}^{k}\left[\frac{\left\{\dot p^k_{Am}\right\}\xi^k_{t,u}u^{-1/3}s_{u,w}}{\frac{\dot c^k d\psi}{u^\chi}+\left(d\psi+[E^k_m]\right)p_{t,u}}\right]du\ dk\ dq\ dw\ dt \end{aligned} \tag{D4}$$

And the total amount of energy preyed by all predators on all consumer organisms in the range of structural volume $[w, w+dw]$ at time t during dt in 1 m^3 of water is

$$\mathrm{E}^{/p}_{t,/w}\ dw\ dt = \frac{\widehat{\xi}^p_{t,w}}{\kappa_X}\int_{k=V_b}^{V^{k\max}_m}\int_{u=V_b}^{k}\left[\frac{\left\{\dot p^k_{Am}\right\}\xi^k_{t,u}u^{-1/3}s_{u,w}}{\frac{\dot c^k d\psi}{u^\chi}+(d\psi+\left[E^k_m\right])p_{t,u}}\right]du\ dk\ dw\ dt \tag{D5}$$

Given this equation, the calculation of the instantaneous mortality rates (Eqs. (12) and (13)) is straightforward.

The ageing mortality: calculation of $a^k_{t,V}$:

Replacing the functional response $f^k_{t,V}$ by its mean value $\bar f$ during the time interval $[0, t]$, Eq. (14) can be integrated to estimate the mean structural volume V_t at age t:

$$V^k_t = \left(\frac{\kappa\left\{\dot p^k_{Am}\right\}\bar f-\left(\kappa\{\dot p^k_{Am}\}\bar f-[\dot p_M]V^{1/3}_{egg}\right)e^{\frac{-[\dot p_M]}{3\left(\kappa\bar f[E_m]^k+[E_G]\right)}t}}{[\dot p_M]}\right)^3 \tag{D6}$$

This formula is inverted to estimate the mean time taken by an individual of species k to reach size (structural volume) V:

$$t^k_V = \frac{-3(\kappa\bar f[E_m]^k+[E_G])}{[\dot p_M]}\ln\left(\frac{\kappa\{\dot p^k_{Am}\}\bar f-[\dot p_M]V^{1/3}}{\kappa\{\dot p^k_{Am}\}\bar f-[\dot p_M]V^{1/3}_{egg}}\right) \tag{D7}$$

This is in turn substituted in Eq. (19) to estimate the mean ageing mortality rate for species k at size (structural volume) V

$$a^k_V = \frac{\ddot h_a}{V_t}\left(\int_{t_1=0}^{t_1=t^k_V}V_{t_1}dt_1 - V_{egg}t^k_V + \frac{[\dot p_M]}{[E_G]}\int_{t_1=0}^{t_1=t^k_V}\int_{t_2=0}^{t_2=t_1}V_{t_2}dt_2dt_1\right) \tag{D8}$$

which, after integration, gives:

$$\begin{aligned} a^k_V = \frac{\ddot h_a}{V_t}\Big[& a^3t^k_V - \tfrac{1}{c}\left(3a^2de^{ct^k_V} - \tfrac{3}{2}ad^2e^{2ct^k_V} + \tfrac{1}{3}d^3e^{3ct^k_V}\right) \\ & + \frac{1}{c}\left(3a^2d - \frac{3}{2}ad^2 + \frac{1}{3}d^3\right) + V_{egg}t^k_V \\ & + \frac{[\dot p_M]}{[E_G]}\left[\tfrac{a^3}{2}t^{k2}_V - \tfrac{1}{c^2}\left(3a^2de^{ct^k_V} - \tfrac{3}{4}ad^2e^{2ct^k_V} + \tfrac{1}{9}d^3e^{3ct^k_V}\right)\right. \\ & \left. + \frac{1}{c}\left(3a^2d - \frac{3}{2}ad^2 + \frac{1}{3}d^3\right)t^k_V + \frac{1}{c^2}\left(3a^2d - \frac{3}{4}ad^2 + \frac{1}{9}d^3\right)\right]\Big] \end{aligned} \tag{D9}$$

with

$$\begin{cases} a = \frac{\kappa [\dot{p}^k_{Am}] \bar{f}}{[p_M]} \\ b = V_{egg}^{1/3} \\ c = \frac{-[\dot{p}_M]}{3(\kappa \bar{f}[E^k_m] + [E_G])} \\ d = a - b \end{cases}$$

Appendix E. From one consumer species to an infinitely diversified community of consumers

Eq. (7) can be integrated over the range of species larger than V

$$\begin{aligned} \int_{k=V}^{k_{\max}} \frac{\partial \xi^k_{t,V}}{\partial t} dk = & - \int_{k=V}^{k_{\max}} \frac{\partial \left(\gamma^k_{t,V} \xi^k_{t,V} \right)}{\partial V} dk \\ & + \int_{k=V}^{k_{\max}} \left(\frac{\gamma^k_{t,V} \xi^k_{t,V}}{V\left(d\psi + f^k_{t,V}[E^k_m] \right)} \left(d\psi + \left[E^k_m \right] \left(V \frac{\partial f^k_{t,V}}{\partial V} + f^k_{t,V} \right) \right) \right) dk \\ & - \int_{k=V}^{k_{\max}} \left(\lambda^k_{t,V} + a^k_{t,V} + s^k_{t,V} + z^k_{t,V} \right) \xi^k_{t,V} dk \end{aligned} \tag{E1}$$

$$\text{Since} \begin{cases} F(x) = \int_{y=x}^{+\infty} f(x,y) dy \\ \frac{dF(x)}{dx} = \int_{y=x}^{+\infty} \frac{\partial f(x,y)}{\partial x} dy - f(x,x) \end{cases} \tag{E2}$$

$$\text{we have } \frac{\partial}{\partial V} \int_{k=V}^{+\infty} (\gamma^k_{t,V} \xi^k_{t,V}) dk = \int_{k=V}^{+\infty} \frac{\partial (\gamma^k_{t,V} \xi^k_{t,V})}{\partial V} dk - \overbrace{\gamma^V_{t,V} \xi^V_{t,V}}^{=0} \tag{E3}$$

This is used to obtain Eq. (22).

Appendix F. Numerical approximations

- Numerical approximation of Eq. (1)
  A semi-implicit approximation of Eq. (1) is derived as follows:

$$\begin{aligned} \Gamma^p_{t+\delta} &= \Gamma^p_t + \delta t \left(r_p \Gamma^p_t \left(1 - \frac{\Gamma^p_{t+\delta t}}{pcc_{t+\delta t}} \right) - \int_{V_0}^{V_1} \lambda^p_{t,V} \xi^p_{t,V} dV \right) \\ &= \Gamma^p_t + \delta t r_p \Gamma^p_t - \frac{\delta t r_p \Gamma^p_t \Gamma^p_{t+\delta t}}{pcc_{t+\delta t}} - \delta t \int_{V_0}^{V_1} \lambda^p_{t,V} \xi^p_{t,V} dV \\ \Leftrightarrow \Gamma^p_{t+\delta} &= \frac{\Gamma^p_t + \delta t \left(r_p \Gamma^p_t - \int_{V_0}^{V_1} \lambda^p_{t,V} \xi^p_{t,V} dV \right)}{1 + \delta t \frac{r_p \Gamma^p_t}{pcc_{t+\delta t}}} \\ \Rightarrow \quad \xi^p_{t+\delta t,V} &= \frac{1}{V \ln\left(\frac{V_1}{V_0} \right)} \left(\frac{\Gamma^p_t + \delta t \left(r_p \Gamma^p_t - \int_{V_0}^{V_1} \lambda^p_{t,V} \xi^p_{t,V} dV \right)}{1 + \delta t \frac{r_p \Gamma^p_t}{pcc_{t+\delta t}}} \right) \\ & \forall V \in [V_0; V_1] \end{aligned} \tag{F1}$$

- Numerical approximation of Eq. (7)
  Fish communities encompass very different species covering a large range of potential sizes ranging approximately from the mean size of fish eggs (10^{-3} m, 10^{-8} kg) to the maximum size of the largest fish predator (4 m and more than 650 kg for giant bluefin tuna or swordfish for instance). To account accurately for growth and predation processes over such a large range of size (structural volume) would require approximating numerically the model with an extremely small resolution over an extremely large number of size intervals. Alternately, a base α log scale can be used to ensure that processes are considered at the proper resolution whatever the size of organisms is while keeping a limited number of weight classes. Using such a size-based log scale can be done by defining

$$\varpi = \frac{\ln(l-\beta)}{\ln(\alpha)} - \gamma = \frac{\ln(a^{-1/3} V^{1/3} - \beta)}{\ln(\alpha)} - \gamma \Leftrightarrow V = a(\alpha^{\varpi+\gamma} + \beta)^3 \tag{F2.}$$

with l the organisms length, α and β being fixed parameters and $\varpi = \{1,2,3,\ldots,n\}$. To be able to choose easily the grid characteristics, the parameters β and γ are expressed in terms of $l_{\min}$ and $l_{\max}$ respectively which are fixed so that the grid depends only on α In the present theoretical study, we arbitrarily decided to focus on large consumer organisms such as fish ranging from 1 mm to 2 m. Accordingly, α is set at 1.04 which corresponds to grid cells varying from 1.5 mm for the smallest size class to 75 mm for the largest class. An irregular grid is derived calculating structural volume steps δV_i so that each grid point V_i is placed at the middle of its associated grid cell.

The model is integrated numerically along 100 length/structural volume classes from $l_{\min} = 10^{-5}$ m to $l_{\max} = 2$ m. For the sake of simplicity, producers are supposed to include phytoplankton and zooplankton. Their biomass is assumed to be distributed over structural volume according to a power law with a constant exponent -1 and to range from 10^{-4} m to 2×10^{-3} m so that there is a slight overlap with the consumer size range.

The system is solved over the species dimension k by solving Eq. (7) for the 100 "numerical species" of the k discretization, at each time step. All of this is done as follows:

$$\begin{aligned} & \forall k \in \{V^{k_1}_m,\ V^{k_2}_m,\ V^{k_3}_m,\ \ldots,\ V^{k_{100}}_m\} \\ & \begin{cases} V = V^k_b & \xi^k_{t+\delta t,V_b} = \xi^k_{t,V_b} + \delta t \left(\frac{\dot{r}^k_t - \dot{\gamma}^k_{t,V_b} \xi^k_{t,V_b}}{\delta V_{V_b}} - \left(\dot{\lambda}^k_{t,V_b} + \dot{a}^k_{t,V_b} + \dot{s}^k_{t,V_b} + \dot{z}^k_{t,V_b} \right) \xi^k_{t,V_b} \right) \\ \forall V \in]V^k_b, k[& \xi^k_{t+\delta t,V} = \xi^k_{t,V} + \delta t \begin{pmatrix} \frac{\dot{\gamma}^k_{t,V-\delta V_V} \xi^k_{t,V-\delta V_V} - \dot{\gamma}^k_{t,V} \xi^k_{t,V}}{\delta V_V} \\ + \frac{\dot{\gamma}^k_{t,V} \xi^k_{t,V}}{V(d\psi + f_{t,V}[E^k_m])} \left(d\psi + \left[E^k_m \right] \left(V \frac{f^k_{t,V} - f^k_{t,V-\delta V_V}}{\delta V_V} + f_{t,V} \right) \right) \\ -(\dot{\lambda}^k_{t,V} + \dot{a}^k_{t,V} + \dot{s}^k_{t,V} + \dot{z}^k_{t,V}) \xi^k_{t,V} \end{pmatrix} \\ V = k & \xi^k_{t+\delta t,V} = \xi^k_{t,V} + \delta t \begin{pmatrix} \frac{\dot{\gamma}^k_{t,V-\delta V_V} \xi^k_{t,V-\delta V_V}}{\delta V_V} \\ + \frac{\dot{\gamma}^k_{t,V} \xi^k_{t,V}}{V(d\psi + f_{t,V}[E^k_m])} \left(d\psi + \left[E^k_m \right] \left(V \frac{f^k_{t,V} - f^k_{t,V-\delta V_V}}{\delta V_V} + f_{t,V} \right) \right) \\ -(\dot{\lambda}^k_{t,V} + \dot{a}^k_{t,V} + \dot{s}^k_{t,V} + \dot{z}^k_{t,V}) \xi^k_{t,V} \end{pmatrix} \end{cases} \end{aligned} \tag{F3}$$

References

Abrams, P.A., 2011. Simple life-history: responses to enrichment and harvesting in systems with intraguild predation. Am. Nat. 178, 305–319.

Andersen, K.H., Beyer, J.E., 2006. Asymptotic size determines species abundance in the marine size spectrum. Am. Nat. 168, 54–61.

Andersen, K.H., Beyer, J.E., Lundberg, P., 2009. Trophic and individual efficiencies of size-structured communities. Proc. R. Soc. B 276, 109–114.

Arino, O., Shin, Y.-J., Mullon, C., 2004. A mathematical derivation of size spectra in fish populations. Comptes Rendus de l'Acade´mie des Sciences. Section Biologies, CRAS 327, 245–254.

Bakun, A., 2006. Wasp-waist populations and marine ecosystem dynamics: navigating the "predator pit" topographies. Prog. Oceanogr. 68, 271–288.

Bakun, A., Weeks, S., 2006. Adverse feedback sequences in exploited marine systems. Fish Fisher. 7, 316–333.

Bakun, A., 2009. Research challenges in the twenty-first century. In: Checkley, D.J., Alheit, Y., Oozeki, Roy, C. (Eds.), IN Climate change and Small Pelagic Fish. Cambridge University Press, Cambridge, pp. 372.

Bax, N.J., 1998. The significance and prediction of predation in marine fisheries. ICES J. Mar. Sci. 55, 997–1030.

Becco, C., Vandewalle, N., Delcourt, J., Poncin, P., 2006. Experimental evidences of a structural and dynamical transition in fish school. Physica A 367, 487–493.

Benoit, E., Rochet, M.J., 2004. A continuous model of biomass size spectra governed by predation and the effects of fishing on them. J. Theor. Biol. 226, 9–21.

Blanchard, J.L., Jennings, S., Law, R., Castle, M.D., McCloghrie, P., Rochet, M.-J., Benoît, E., 2009. How does abundance scale with body size in coupled size-structured food webs? J. Anim. Ecol. 78, 270–280.
Block, B.A., Costa, D.P., Boehlert, G.W., Kochevar, R.E., 2003. Revealing pelagic habitat use: the tagging of Pacific pelagics program. Oceanol. Acta 25, 255–266.
Blueweiss, L., Fox, H., Kudzma, V., Nakashima, D., Peters, R., Sams, S., 1978. Relationships between body size and some life history parameters. Oecologia 37, 257–272.
Bruggeman, J., Kooijman, S.A.L.M., 2007. A biodiversity-inspired approach to aquatic ecosystem modeling. Limnol. Oceanogr. 52, 1533–1544.
Clarke, A., Johnston, N.M., 1999. Scaling of metabolic rate with body mass and temperature in teleost fish. J. Anim. Ecol. 68, 893–905.
Clarke, A., Fraser, K.P.P., 2004. Why does metabolism scale with temperature? Funct. Ecol. 18, 243–251.
Clarke, A., 2004. Is there a universal temperature dependence of metabolism? Funct. Ecol. 18, 252–256.
Cushing, J.M., 1992. A size-structured model for cannibalism. Theor. Pop. Biol. 42, 347–361.
Czirok, A., Vicsek, T., 2000. Collective behavior of interacting self-propelled particles. Physica A 281, 17–29.
Datta, S., Delius, G.W., Law, R., Plank, M.J., 2011. A stability analysis of the power-law steady state of marine size spectra. J. Math. Biol. 72, 1361–1382.
Dickie, L.M., Kerr, S.R., Boudreau, P.R., 1987. Size-dependent processes underlying regularities in ecosystem structure. Ecol. Monogr. 57 (3), 233–250.
Edvardsen, A., Zhou, M., Tande, K.S., Zhu, Y., 2002. Zooplankton population dynamics: measuring in situ growth and mortality rates using an Optical Plankton Counter. Mar. Ecol. Prog. Ser. 227, 205–219.
Enquist, B.J., Economo, E.P., Huxman, T.E., Allen, A.P., Ignace, D.D., Gillooly, J.F., 2003. Scaling metabolism from organisms to ecosystems. Nature 423, 639–642.
Essington, T.E., Schindler, D.E., Olson, R.J., Kitchell, J.F., Boggs, C., Hilborn, R., 2002. Alternative fisheries and the predation rate of Yellowfin Tuna in the Eastern Pacific Ocean. Ecol. Appl. 12 (3), 724–734.
Follows, M.J., Dutkiewicz, S., Grant, S., Chisholm, S.W., 2007. Emergent biogeography of microbial communities in a model ocean. Science 315, 1843–1846.
Fonteneau, A., Lucas, V., Tewkai, E., Delgado, A., Demarcq, H., 2008. Meso-scale exploitation of a major tuna concentration in the Indian Ocean. Aquat Living Resour 21 (2), 109–121.
Fossheim, M., Zhou, M., Tande, K.S., Pedersen, O.-P., Zhu, Y., Edvardsen, A., 2005. Interactions between biological and environmental structures along the coast of northern Norway. Mar. Ecol. Prog. Ser. 300, 147–158.
Fréon, P., Misund, O., 1999. Dynamics of pelagic fish distribution and behaviour: effects on fisheries and stock assessment, Fishing News Books. Blackwell Science, Oxford 348 p.
Froese, R., Pauly, D., 2000. FishBase 2000: concepts, design and data sources. ICLARM, Los Baños, Laguna, Philippines 344p.
Fulton, E.A., Fuller, M., Smith, A.D.M., Punt, A.E., 2004. Ecological Indicators of the Ecosystem Effects of Fishing: Final Report. Australian Fisheries Management Authority Report, R99/1546. 239 pp.
Gautrais, J., Jost, C., Theraulaz, G., 2008. Key behavioural factors in a self-organised fish school model. Ann. Zool. Fennici. 45, 415–428.
Gillooly, J.F., Brown, J.H., West, G.B., Savage, V.M., Charnov, E.L., 2001. Effects of size and temperature on metabolic rate. Science 293, 2248–2251.
Gillooly, J.F., Charnov, E.L., West, G.B., Savage, V.M., Brown, J.H., 2002. Effects of size and temperature on developmental time. Nature 417, 70–73.
Hartvig, M., Andersen, K., Beyer, J., 2011. Food web framework for size-structured populations. J. Theor. Biol. 272, 113–122.
ICCAT, 2009. ICCAT Manual. International Commission for the Conservation of Atlantic Tuna. In: ICCAT Publications [on-line]. ISBN (Electronic Edition): 978-92-990055-0-7.
Jennings, S., Pinnegar, J.K., Polunin, N.V.C., Boon, T., 2001. Weak cross-species relationships between body size and trophic level belie powerful size-based trophic structuring in fish communities. J. Anim. Ecol. 70, 934–944.
Jennings, S., Pinnegar, J.K., Polunin, N.V.C., Warr, K.J., 2002. Linking size-based and trophic analyses of benthic community structure. Mar. Ecol. Prog. Ser. 226, 77–85.
Jennings, S., 2005. Size-based analysis of aquatic food webs. In: Belgrano, A., Scharler, U.M., Dunne, J., Ulanowicz, R.E. (Eds.), Aquatic food webs: an ecosystem approach. Oxford University Press, Oxford, pp. 86–97.
Jiménez, F., Rodriguez, J., Jimenez-Gomez, F., Bautista, B., 1989. Bottlenecks in the propagation of a fluctuation up the planktonic size spectrum in Mediterranean coastal waters. In: Ros, J.D. (Ed.), Topics in Marine Biology, 53. Scientia Marina, pp. 269–275.
Kooi, B.W., Kelpin, F.D.L., 2003. Physiologically structured population dynamics: a modeling perspective. Comments Theor. Biol. 8, 125–168.
Kooijman, S.A.L.M., 1986. Energy budgets can explain body size relations. J. Theor. Biol. 121, 269–282.
Kooijman, S.A.L.M., 2000. Dynamic Energy and Mass Budgets in Biological Systems, Second Ed. Cambridge University Press, Cambridge 424p.
Kooijman, S.A.L.M., 2010. Dynamic Energy and Mass Budgets in Biological Systems. Cambridge University Press, Cambridge. Third Ed. 514p.
van Leeuwen, I.M.M., Vera, J., Wolkenhauer, O., 2010. Dynamic Energy Budget approaches for modeling organismal ageing. Proc. R. Soc. B. 365, 3443–3454.
Levy, D.A., Wood, C.C., 1992. Review of proposed mechanisms for sockeye salmon cycles in the Fraser River. J. Math. Biol. 54, 241–261.
Macpherson, E., Gordoa, A., 1996. Biomass spectra in benthic fish assemblages in the Benguela system. Mar. Ecol. Prog. Ser. 138, 27–32.
Makris, N.C., Ratilal, P., Jagannathan, S., Gong, Z., Andrews, M., Bertsatos, I., Godø, O.R., Nero, R.W., Jech, J.M., 2009. Critical population density triggers rapid formation of vast oceanic fish shoals. Science 323, 1734–1737.
Marquet, P.A., Quiñones, R.A., Abades, S., Labra, F., Tognelli, M., Arim, M., Rivadeneira, M., 2005. Scaling and power-laws in ecological systems. J. Exp. Biol. 208, 1749–1769.
Maury, O., Faugeras, B., Shin, Y-J., Poggiale, J.C., Ben Ari, T., Marsac, F., 2007a. Modelling environmental effects on the size-structured energy flow through marine ecosystems. Part 1: the model. Prog. Oceanogr. 74 (4), 479–499.
Maury, O., Shin, Y-J., Faugeras, B., Ari, T.Ben, Marsac, F., 2007b. Modeling environmental effects on the size-structured energy flow through marine ecosystems. Part 2: simulations. Prog Oceanogr 74 (4), 500–514.
Maury, O., 2010. An overview of APECOSM, a spatialized mass balanced "Apex Predators ECOSystem Model" to study physiologically structured Tuna population dynamics in their ecosystem. In: John St, M., Monfray, P. (Eds.), Parameterisation of Trophic Interactions in Ecosystem Modelling, 2010. Prog. Oceanogr., pp. 113–117.
Ménard, F., Lorrain, A., Potier, M., Marsac, F., 2007. Isotopic evidence of distinct feeding ecologies and movement patterns in two migratory predators (yellow-fin tuna and swordfish) of the western Indian Ocean. Mar. Biol. 153 (2), 141–152.
Metz, J.A.J., Dieckman, O., 1986. The dynamics of physiologically structured populations. Lecture notes in biomathematics, vol. 68. Springer Verlag, Berlin.
Moloney, C., Jarre, A., Kimura, S., Mackas, D.L., Maury, O., Murphy, E.J., Peterson, W.T., Runge, J.A., Tadokoro, K., 2010. Dynamics of marine ecosystems: ecological processes. In: Barange, M., Field, J., Harris, R., Hofmann, E., Perry, I., Werner, C. (Eds.), GLOBEC International Synthesis Book: Global Change and Marine Ecosystems. Oxford University Press, pp. 412, p.
Moyle, P.B., Cech, J.J., 2004. Fishes, An Introduction to Ichthyology, Fifth Ed. Prentice Hall, Benjamin Cummings 726 pp.
Nisbet, R.M., Muller, E.B., Lika, K., Kooijman, S.A.L.M., 2000. From molecules to ecosystems through dynamic energy budget models. J. Anim. Ecol. 69, 913–926.
Nisbet, R.M., Mc Cauley, E., 2010. Dynamic Energy Budget theory and population ecology: lessons from daphnia. Proc. R. Soc. B 365, 3541–3552.
Ogut, H., Reno, P., 2004. Prevalence of Furunculosis in Chinook Salmon depends on density of the host exposed by cohabitation. N. Am. J. Aquaculture 66, 191–197.
Pauly, D., Christensen, V., Walters, C., 2000. Ecopath, Ecosim, and Ecospace as tools for evaluating ecosystem impact of fisheries. ICES J Mar Sci 57, 697–706.
Platt, T., Denman, K., 1978. The structure of pelagic marine ecosystems. Rapp. Procés-Verbaux des Réunions du Conseil International d'Exploration de la Mer 173, 60–65.
Platt, T., Denman, K., 1997. Organisation in the pelagic ecosystem. Helgol. Wiss. Meeresunters 30, 575–581.
Polovina, J.J., 1984. Model of a coral reef ecosystem. I: the ECOPATH model and its application to French Frigate Schoals. Coral Reefs 3, 1–11.
Pörtner, H.O., 2002. Physiological basis of temperature-dependent biogeography: trade-offs in muscle design and performance in polar ectotherms. J. Exp. Biol. 205, 2217–2230.
Potier, M., Marsac, F., Cherel, Y., Lucas, V., Sabatié, R., Maury, O., Ménard, F., 2007. Forage fauna in the diet of three large pelagic fish (lancetfish, swordfish, and yellowfin tuna) in the western equatorial Indian Ocean. Fish. Res. 83, 60–72.
Quiñones, R.A., Platt, T., Rodríguez, J., 2003. Patterns of biomass size-spectra from oligotrophic waters of the Northwest Atlantic. Prog. Oceanogr. 57, 405–427.
De Roos, A.M., 1997. A gentle introduction to physiologically structured population models. In: Tuljapurkar, S., Caswell, H. (Eds.), Structured-population models in marine, terrestrial, and freshwater systems. Chapman & Hall, pp. 643.
Sheldon, R.W., Prakash, A., Sutcliffe, W.H., 1972. The size distribution of particles in the ocean. Limnol. Oceanogr. 17 (3), 327–340.
Shin, Y.-J., Cury, P., 2004. Using an individual-based model of fish assemblages to study the response of size spectra to changes in fishing. Can. J. Fish. Aquat. Sci. 61, 414–431.
Silvert, W., Platt, T., 1978. Energy flux in the pelagic ecosystem: a time-dependent equation. Limnol. Oceanogr. 23, 813–816.
Silvert, W., Platt, T., 1980. Dynamic energy flow model of the particle size distribution in pelagic ecosystems. In: Kerfoot, W. (Ed.), Evolution and Ecology of Zooplancton Communities. University Press of New England, Illanover, NH, pp. 754–763.
Sousa, T., Domingos, T., Poggiale, J.C., Kooijman, S.A.L.M., 2010. Formalized DEB theory restores coherence in core biology. Proc. R. Soc. B 365, 3413–3428.
Speakman, J.R., 2005. Body Size, Energy Metabolism and Lifespan. J. Exp. Biol. 208, 1717–1730.
Thygesen, U., farnsworth, K., Andersen, K., Beyer, J., 2005. How optimal life history changes with the community size-spectrum. Proc. R. Soc. B. 272, 1323–1331.
Tu, Y., 2000. Phases and phase transition in flocking systems. Physica A 281, 30–40.
Tuljapurkar, S., Caswell, H., 1997. Structured-population models in marine, terrestrial, and freshwater systems. Chapman & Hall 643p.
Vergnon, R., Shin, Y.-J., Cury, P., 2009. Cultivation, Allee effect and resilience of large demersal fish populations. Aquat. Living Resour. 21, 287–295.

Vicsek, T., Czirok, A., Ben-Jacob, E., Cohen, I., Shochet, O., 1995. Novel type of phase transition in a system of self-driven particles. Phys. Rev. Lett. 75 (6), 1226.
Walters, C., Christensen, V., Pauly, D., 1997. Structuring dynamic models of exploited ecosystems from trophic massbalance assessments. Rev. Fish Biol. Fisher. 7 (2), 139–172.
Walters, C., Kitchell, J.F., 2001. Cultivation/depensation effects on juvenile survival and recruitment: implications for the theory of fishing. Can. J. Fish. Aquat. Sci. 58, 39–50.
Weimerskirch, H., Le Corre, M., Jaquemet, S., Potier, M., Marsac, F., 2004. Foraging strategy of a top predator in tropical waters: great frigatebirds in the Mozambique Channel. Mar. Ecol. Prog. Ser. 275, 297–308.
White, E.P., Morgan Ernest, S.K., Kerkhoff, A.J., Enquist, B., 2007. Relationships between body size and abundance in ecology. Tree 22 (6), 323–330.
Woodward, G., Ebenman, B., Emmerson, M., Montoya, J.M., Olesen, J.M., Valido, A., Warren, P.H., 2005. Body size in ecological networks. Trends Ecol. Evolut. 20 (7), 402–409.
Young, J.W., Bradford, R., Lamb, T.D., Clementson, L.A., Kloser, R., Galea, H., 2001. Yellowfin tuna (Thunnus albacares) aggregations along the shelf break off south-eastern Australia: links between inshore and offshore processes. Mar. Freshwater Res. 52, 463–474.
Zhou, M., Huntley, M.E., 1997. Population dynamics theory of plankton based on biomass spectra. Mar. Ecol. Prog. Ser. 159, 61–73.